Synaptic input from CA3 pyramidal cells to dentate basket cells in rat hippocampus

Tracy B. Kneisler* and Raymond Dingledine

*Department of Pharmacology, Emory University, Atlanta, GA 30322 and *Department of Pharmacology, University of North Carolina at Chapel Hill, NC 27599, USA*

1. Excitatory inputs from CA3 pyramidal cells to dentate basket cells were examined using the whole-cell recording technique in neonatal (10–16 days) rat hippocampal slices to characterize this unexpected feedback pathway.

2. Minimal electrical stimulation of the CA3 pyramidal layer evoked in basket cells short latency (5·2 ± 0·4 ms) glutamate receptor-mediated excitatory postsynaptic currents (EPSCs) with fast rise times (at −70 mV, 0·9 ± 0·2 ms), fast decay time constants (3·6 ± 0·6 ms), and small amplitudes (−14 ± 3·4 pA). Minimal electrical stimulation evoked monosynaptic EPSCs in only 48 ± 9·2% of the trials suggesting that the CA3 pyramidal cell to basket cell pathway was unreliable.

3. CA3 pyramidal cell layer stimulation did not antidromically or synaptically activate granule cells but did evoke polysynaptic IPSCs in granule cells, suggesting that the net effect of CA3 pyramidal cell firing on the dentate gyrus was granule cell inhibition.

4. Stimulation of the CA3 pyramidal cell layer evoked both monosynaptic and polysynaptic EPSCs in basket cells, which were eliminated by a knife lesion separating CA3 from the dentate gyrus. The latencies of the EPSCs evoked in 0·6 mM extracellular calcium were the same as the earliest latencies of EPSCs in 1·5 mM calcium, suggesting that those EPSCs were monosynaptic. The polysynaptic input was more prominent in the presence of 10 μM bicuculline, implying that inhibitory GABAergic circuits normally limit this feedback from CA3 to basket cells.

5. In recordings from 103 pairs of CA3 pyramidal cells and dentate basket cells from 11 slices, two polysynaptic connections were found that were active only when the presynaptic CA3 pyramidal neuron fired in bursts. No monosynaptic connections between CA3 pyramidal cells and basket cells were identified indicating that connections between the two cell types may be sparse.

6. Raising the external potassium concentration from 3·5 to 8·5 mM, which elicited burst firing in CA3 pyramidal cells, resulted in a barrage of EPSCs and action potentials in basket cells. In contrast, granule cells neither fired action potentials nor exhibited increased EPSC frequency in elevated potassium but instead received a higher frequency of bicuculline-sensitive IPSCs, consistent with interneuron firing. The CA3 pyramidal cell to basket cell monosynaptic pathway exhibited paired-pulse facilitation as manifested by an increased probability of release, which supports the idea that basket cells were better activated by short trains of action potentials than by single inputs.

7. The mode of spontaneous EPSP amplitudes for basket cells was 0·4 ± 0·1 mV. Since the resting membrane potential of basket cells was about 10 mV from their firing threshold, up to twenty-five nearly simultaneous EPSPs may be required to evoke an action potential. These data suggest that this pathway would effectively activate basket cells when several pyramidal cells fired synchronously or a single cell fired repetitively.

8. We conclude that monosynaptic and polysynaptic feedback from CA3 onto dentate basket cells provides CA3 pyramidal cells with a means to regulate the strength of their mossy fibre input. The CA3 pathways to basket cells may regulate the signal-to-noise ratio for information proceeding through dentate gyrus into the hippocampus by reducing mossy fibre input to CA3 when CA3 pyramids are burst firing.

Synchronous firing of CA3 pyramidal neurons is involved in both epileptic interictal activity (Traub & Miles, 1991) and, in milder form, new memory formation (Buzsaki, 1989). Regulation of hippocampal CA3 pyramidal cell excitability is thus critical for normal brain function. The type and intensity of information relayed to the CA3 region via the perforant path–mossy fibre system is controlled by granule cell excitability, which is itself restricted by a high granule cell spike threshold and local inhibition by a variety of interneurons that include dentate basket cells.

To appreciate how interneurons regulate information flow through the hippocampus, it is necessary to identify and characterize the reliability and strengths of their inputs, and to understand the physiological conditions or presynaptic firing patterns that strongly engage the various interneuron populations. The roles of interneurons in hippocampal circuitry are becoming better understood as these issues are explored by a combination of electrophysiological and morphological approaches. CA3 pyramidal cells make single contacts with target interneurons and appear to release only a single quantum per event (Gulyas, Miles, Sik, Toth, Tamamaki & Freund, 1993). In turn, interneurons in the CA1 and dentate regions form up to twelve synaptic contacts with each target pyramidal neuron or granule cell (Buhl, Halasy & Somogyi, 1994). The view is emerging of a paucity of synaptic inputs to interneurons from individual pyramidal or granule cells, raising the question of whether firing of a single principal cell is sufficient to activate interneurons (e.g. Stevens, 1994).

Anatomical and physiological data suggest that basket cells in the dentate gyrus contribute to both feedforward and feedback inhibition of granule cells. Basket cells in the dentate gyrus immunostain for GABA (Sloviter & Nilaver, 1987) and glutamic acid decarboxylase (GAD) (Ribak, Vaughn & Saito, 1978; Seress & Ribak, 1983), express two forms of GAD mRNA (Houser & Esclapez, 1994), and form symmetric synapses (Seress & Ribak, 1983; Seress & Frotscher, 1991), all features of inhibitory neurons. Although electrophysiological recordings from basket cells are scarce, and no detailed physiological study of the efferent or afferent connections of these cells has been published, interneurons located in the granule cell layer can be excited by perforant path stimulation (Scharfman & Schwartzkroin, 1990) and by granule cells (Scharfman, Kunkel & Schwartzkroin, 1990). Anatomical data suggest that basket cells receive their input primarily from granule cells (Seress & Ribak, 1990; Ribak & Peterson, 1991) and project primarily to granule cells (Seress & Ribak, 1983).

Information flow through the hippocampus has long been considered unidirectional: excitatory impulses are propagated from entorhinal cortex to granule cells by the perforant path, then to CA3 pyramidal cells via mossy fibres, onto CA1 pyramidal cells by Schaffer collaterals, and from CA1 pyramidal cells into the subiculum. Recent reports, however, suggest that information in the hippocampus can be conveyed from one region to another in either direction. Anatomical studies (Ishizuka, Weber & Amaral, 1990; Li, Somogyi, Ylinen & Buzsaki, 1994) have shown that some CA3 pyramidal cell axons ramify extensively in the hilus and molecular layer of the dentate gyrus, but the targets of those axons were not identified. A recent study (Sik, Ylinen, Penttonen & Buzsaki, 1994) demonstrated that some interneurons in alveus and stratum oriens of CA1 project to the dentate gyrus and/or CA3. Scharfman (1994*a*,*b*) demonstrated that in the presence of $GABA_A$ receptor antagonists CA3 pyramidal cells excite mossy cells in the dentate hilus.

We have obtained whole-cell patch clamp recordings from morphologically identified dentate basket cells to examine a long-range feedback pathway from CA3 pyramidal cells in neonatal rats. We identified and characterized monosynaptic and polysynaptic pathways from CA3 pyramidal cells to basket cells and described conditions under which both pathways were strongly activated or potentiated.

Abstracts describing some of this work have appeared previously (Kneisler and Dingledine, 1993, 1994).

METHODS

Male Sprague–Dawley rats, 10–16 days old, were used to prepare 250 μm thick hippocampal slices in ice-cold artificial cerebrospinal fluid (ACSF). Rats were decapitated and the brains removed. Transverse slices from the temporal pole were obtained by slicing along the longitudinal axis of the brain with a Vibratome (Series 1000, Oxford International, St Louis, MO, USA). Slices were incubated at 30 °C for 30–45 min in ACSF oxygenated with 95% O_2 and 5% CO_2, placed in the recording chamber under a platinum-supported nylon mesh, and perfused at a rate of 1–3 ml min^{-1} with room temperature ACSF. ACSF was composed of (mM): 130 NaCl, 24 $NaHCO_3$, 3·5 KCl, 1·25 NaH_2PO_4, 1·5 $CaCl_2.2H_2O$, 1·5 $MgSO_4.7H_2O$ and 10 glucose, pH 7·4, 305–310 mosmol l^{-1}. Extracellular potassium was elevated in some experiments by the addition of 1 M KCl to normal ACSF. Extracellular calcium was decreased to 1·0 or 0·6 mM by reducing $CaCl_2$ in some experiments. All drugs were bath applied in known concentrations. The dead time of the perfusion system was 15–45 s. Drug responses were recorded after at least 7 min of perfusion. Unless stated otherwise, all experiments except those which examined IPSCs were performed in the presence of 10 μM bicuculline methobromide to block $GABA_A$-mediated inhibition.

Current and voltage recordings of seventy-two dentate basket cells and fourteen granule cells were made for this study using standard whole-cell patch clamp techniques (Edwards, Konnerth, Sakmann & Takahashi, 1989). Unpolished patch electrodes used for voltage clamp recordings were fabricated from borosilicate glass (World Precision Instruments, Inc., Sarasota, FL, USA) and had resistances of 4–6 MΩ when filled with internal solution containing (mM): 140 methanesulphonic acid, 10 Hepes, 2 $MgCl_2$ and 130 CsOH (buffered to pH 7·3 with CsOH and adjusted to 270–275 mosmol l^{-1} with water). Similar patch pipettes were used for current clamp recordings except that KOH replaced CsOH in the internal solution so that action potential properties could be

better assessed. Biocytin (0·4%, Sigma) was also included in the internal solution for visualization of neurons following recording. The recording electrode was manoeuvred under visual control into the dentate gyrus where individual cell bodies were visually identified using Hoffman optics (total magnification ×600), and tight seals (> 2 GΩ) were obtained while in current clamp mode. Within 1 min after establishing the whole-cell patch clamp configuration, passive membrane properties and action potential amplitudes were examined before switching to voltage clamp mode. Cells accepted for further analysis typically had an initial resting membrane potential greater than −45 mV (mean ± S.E.M., −50 ± 1·8 mV, $n = 31$) for basket cells or −55 mV (−71 ± 2·2 mV, $n = 6$) for granule cells, input resistances greater than 200 MΩ (304 ± 15 MΩ for forty-six basket cells and 250 ± 35 MΩ for five granule cells), series resistances less than 20 MΩ (12 ± 0·4 MΩ for forty-seven basket cells and 14 ± 1·3 for six granule cells), and action potentials that overshot 0 mV. Mean resting membrane potential, input resistance, and series resistance were pooled from cells recorded with both caesium- and potassium-containing electrodes. Dialysis of the cell with caesium generally resulted in stabilization at a more depolarized membrane potential than with potassium as the major cation in the pipette. No cells fired an action potential on the anode break. Series resistance was determined by balancing the 'bridge' while in current clamp mode. Membrane potentials were not compensated for series resistance-induced errors. Cells were typically voltage clamped to −70 mV unless stated otherwise.

Following completion of the experiments, slices were fixed at least overnight in 4% paraformaldehyde in phosphate-buffered saline (PBS: 120 mM NaCl, 2·7 mM KCl and 10 mM phosphate buffer, pH 7·4). Slices then were treated with 0·5% H_2O_2 in PBS for 30 min to remove endogenous peroxidase activity, permeabilized with 0·5% Triton X-100 in PBS, and exposed to a biotin–avidin–horseradish peroxidase complex (Vectastain ABC Kit, Vector Labs, Burlingame, CA, USA) for up to 12 h. Slices were then incubated in 0·56 mM 3,3′-diaminobenzidine tetrahydrochloride and 0·015% H_2O_2 until the cells filled with biocytin began a colorimetric change. After dehydrating with alcohols and clearing with cedarwood oil (Fisher, Pittsburgh, PA, USA), slices were mounted in Permount (Fisher) and imaged. An image analysis program (Image-1, Universal Imaging Corp., West Chester, PA, USA) was used in many instances to provide a 3-D reconstructed image of the stained cell. Some cells could not be identified following the experiment because they were removed from the slice as the recording electrode was removed.

Some whole-cell patch clamp recordings of basket cells were done with simultaneous single unit extracellular recording of granule cells or CA3 pyramidal cells. The extracellular electrode (tip size, ~1 μm) contained 1 M NaCl. Basket cells were voltage clamped as described above, and their membrane current was monitored for synaptic events as the extracellular recording electrode was lowered slowly through the visually identified CA3 pyramidal layer or granule cell layer.

All currents and voltages were recorded using an Axopatch-1A electrometer (Axon Instruments), except extracellular single unit voltage recordings that were recorded using a Grass P15 AC electrometer. Signals were filtered at 1–10 kHz (−3 dB) and were digitized at 7–30 KHz on an IBM compatible 80486 computer using PCLAMP and Axotape data acquisition software (Axon Instruments). Signals were also stored on videotape for later analysis. Data were analysed using a combination of Axotape, routines written in our laboratory for MicroCal Origin software (MicroCal Software, Inc., Northhampton, MA, USA) and the N05 spontaneous event program supplied by Dr Steve Traynelis (Emory University, Atlanta, GA, USA.

Electrical stimulation of CA3 pyramidal cells was applied through an ACSF-filled patch pipette (tip size, ~3–5 μm) positioned 50–150 μm into the cell layer. Stimuli of 10–150 μA (typically 40–100 μA) for 100–200 μs were given every 3–5 s. Stimulus intensity was set as the minimum stimulus necessary to evoke visually identifiable EPSCs. Synaptic failures, defined as no visually significant change in the baseline following an electrical stimulus, were common. Visually selected synaptic failures were averaged, and the mean subtracted from each trace with an identified evoked EPSC to isolate the EPSC from the stimulus artifact. The time from the beginning of the stimulus artifact to the foot of the evoked EPSC was defined as its latency. Paired-pulse potentiation of the monosynaptic pathway was examined by comparing the failure rate and amplitude of the population of EPSCs with the shortest latency following the first and second of paired stimuli presented 40–60 ms apart. The 10–90% rise times of the spontaneous EPSCs and failure-subtracted evoked EPSCs were calculated for individual synaptic events by linear regression, and the decay time constants were fitted by the sum of one or two exponential components using a simplex algorithm and least squares criteria. All rise times, decay time constants, amplitudes and latencies represent the average calculated from 25–130 EPSCs in each cell.

All data are expressed as means ± standard error of the mean. When appropriate, Student's paired or unpaired t tests were performed.

Other drugs used were D-2-amino-phosphonovaleric acid (D-APV), 6-cyano-7-nitro-quinoxaline-2,3-dione (CNQX, Tocris Cookson), bicuculline methobromide, methanesulphonic acid, and 3,3′-diaminobenzidine tetrahydrochloride (Sigma). All salts (99·99% pure) were obtained from Sigma or Aldrich. Premixed PBS was obtained from Sigma.

RESULTS

Morphology and firing properties of basket cells

Seventy-two morphologically and physiologically identified interneurons were examined using the whole-cell patch clamp technique to evaluate the synaptic input from the CA3 pyramidal layer. Of the seventy-two interneurons, thirty-seven were recovered in whole or part for morphological analysis. Multiple cells filled in the same slice were not encountered; since biocytin crosses gap junctions (e.g. Tarenishi & Negishi, 1994), this finding suggests that these cells were probably not connected via gap junctions. We cannot eliminate the possibility, however, that gap junctions exist between those cells that are permeant to molecules smaller than biocytin. All the interneurons recorded for this study had cell bodies at the hilar–granule cell layer interface and dendrites perpendicular to the granule cell layer extending into the molecular layer and hilus. These interneurons were somewhat morphologically heterogeneous. One of the most obvious morphological differences among the interneurons was the number of primary dendrites extending into the molecular layer (Fig. 1*A* and *B*), ranging from one ($n = 15$) to several

($n = 8$). Cells in neonatal rat dentate gyrus with both dendritic patterns and cell body location and size have been described as 'dentate basket cells' by Seress and Ribak (1990). Another difference between the interneurons was the arborization of the axons. Of the twenty-one interneurons in which the axon was filled, three had axons ramifying almost exclusively in the granule cell layer (Fig. 1*D*), eleven had axons ramifying in both the granule cell layer and molecular layer (Fig. 1*C*), and seven had axons ramifying primarily in the molecular and granule

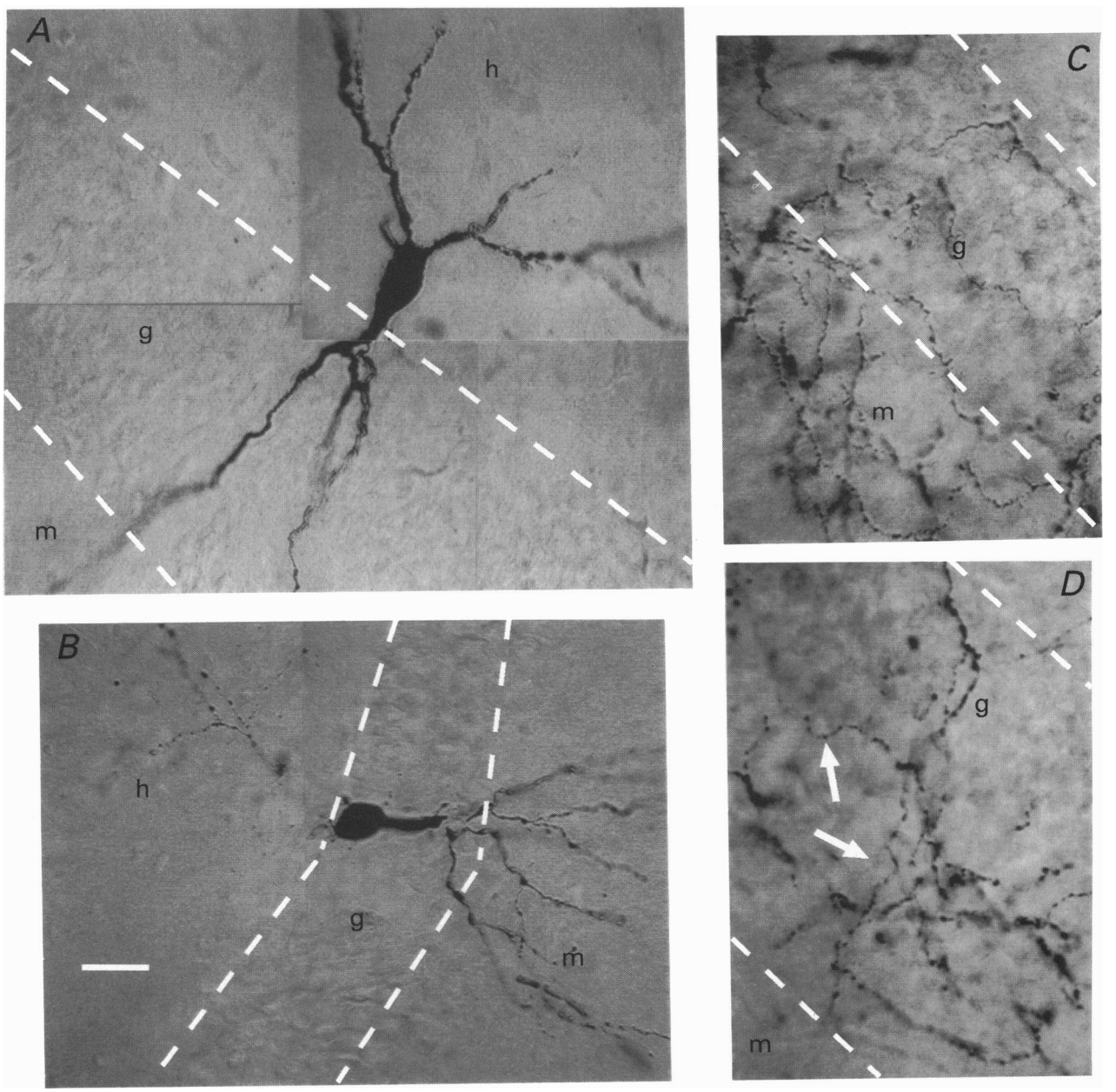

Figure 1. Morphology of interneurons in the granule cell layer

Biocytin-filled interneurons with cell bodies along the hilar border of the granule cell layer were distinguishable based on their cell body size, orientation, number of primary dendrites and axonal arborization. These interneurons, referred to collectively as basket cells, had large cell bodies, were oriented perpendicular to the granule cell layer and had one (*B*) or several (*A*) primary dendrites that extended through the granule cell layer into the molecular layer. In addition, some basket cell axons ramified in the granule cell layer and the molecular layer (*C*), some ramified exclusively within the granule cell layer (*D*), and some axons invaded the granule and molecular layers as well as the hilus (not shown). Basket cell axons occasionally outlined granule cell bodies, presumably forming 'basket-like' synapses (arrows in *D*). Areas in the dentate gyrus are represented as: m, molecular layer; g, granule cell layer; h, hilus. Scale bar represents 25 μm.

layers but also with some arborization in the hilus. Some axons in the granule cell layer seemed to partially encircle individual granule cell bodies (Fig. 1*D*, arrows). Interneurons with axons ramifying primarily in the hilus, as reported for axo-axonic cells (Han, Buhl, Lorinczi & Somogyi, 1993), were not encountered. Interneurons located in the hilus near the granule cell layer that had horizontally oriented cell bodies and dendrites parallel to the granule cell layer were encountered but not included in this study. Because axons were recovered in only twenty-one biocytin-filled interneurons and because the morphology was examined only at the light microscopy level, anatomical classifications based on synapse locations could not be determined. However, previous studies reporting dentate interneuron morphology have identified cells similar to the ones in this study as basket cells (Seress, 1978; Seress & Ribak, 1990; Han *et al.* 1993). Since no physiological differences between the cells used in this study were evident, the dentate interneurons used for this study will be collectively referred to as basket cells.

Basket cells could be distinguished from granule cells by several criteria including morphology, firing pattern, and action potential characteristics. The cell bodies of basket cells were 4–5 times larger than those of granule cells (Fig. 1) and were visually identifiable under Hoffman optics at high power (total magnification ×600). In addition, the basket cell axons that were well stained, ramified in the granule cell layer and molecular layer and never sent granule cell-like axons through the hilus toward the CA3 pyramidal layer. Basket cells and granule cells were also distinguishable by physiological criteria. Basket cells had more depolarized resting membrane potentials (−50 ± 1·8 mV for thirty-one basket cells *vs.* −71 ± 2·2 mV for six granule cells) and lacked spike frequency adaptation (Fig. 2). In addition, basket cells received spontaneous EPSCs at high frequency while granule cells received few spontaneous EPSCs (not shown). In no instance was a physiologically identified basket cell later found by morphological criteria to be a granule cell.

Pathways from CA3 to dentate basket cells

Electrical stimulation of the CA3b or CA3c pyramidal layer evoked EPSCs in basket cells (Fig. 3*A*). Basket cell locations and effective CA3 pyramidal layer stimulation sites are illustrated in Fig. 4*A*. The intensity of the CA3 pyramidal layer stimuli used for these experiments was the minimum necessary to evoke an EPSC in the basket cells. Representative traces from a basket cell during CA3 pyramidal cell stimulation are displayed in Fig. 3*A*. Electrical stimulation of the CA3 pyramidal layer evoked EPSCs in this basket cell only 49% of the time. For this experiment and all others, failures were averaged, and the average was subtracted from individual records so that evoked EPSCs were clearly separated from the stimulus artifacts. The EPSCs were distinguished from failures by amplitudes greater than the recording noise (Fig. 3*C*) and a characteristic fast rising and exponentially decaying shape (Fig. 3*A*). The amplitude of the evoked EPSCs in this basket cell (mean, −9·1 ± 0·8 pA, $n = 26$; mode, −9·2 pA), though variable, was quite small. The EPSCs had moderate 10–90% rise times (1·0 ± 0·2 ms, $n = 26$ EPSCs) and decay time constants of 3·4 ± 0·7 ms ($n = 26$ EPSCs) that were well fitted by a single exponential. The decay of an evoked EPSC from this cell is shown in Fig. 3*B* fitted with a single exponential. The mean 10–90% rise time of EPSCs recorded from nine basket cells was 0·9 ± 0·2 ms, and the mean decay time constant, well fitted by a single exponential, was 3·6 ± 0·6 ms. The average evoked EPSC amplitude from these basket cells was −14 ± 3·4 pA (mode, −14 ± 1·3 pA).

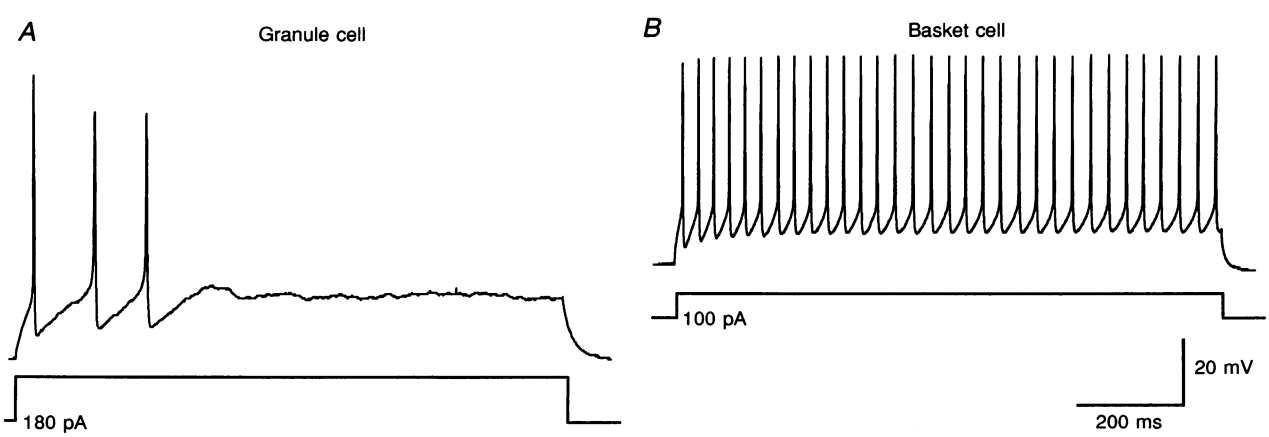

Figure 2. The firing patterns of granule and basket cells differ

A, granule cells, when given a 1 s depolarizing current step, exhibited spike frequency adaptation. This granule cell, resting at −74 mV, fired only three action potentials in response to a 180 pA current injection. *B*, basket cells, on the other hand, showed little or no spike frequency adaptation with a similar 1 s depolarization. This basket cell, which had a resting potential of −60 mV, fired a series of action potentials that showed no adaptation over the 1 s 100 pA current injection.

Although stimulus sites throughout the CA3b and CA3c regions were effective (Fig. 4*A*), we were concerned that stimulus spread into the hilus may have been responsible for the evoked EPSCs in basket cells. To investigate whether stimulus spread to either hilar neurons or granule cells was responsible for the evoked EPSCs, we used the tip of a scalpel blade to cut through the slice perpendicular to the CA3 pyramidal layer either at the CA3b–c border of the dentate gyrus (Fig. 4*B*) or at the CA3c–hilar border. These cuts severed connections between CA3 and the dentate gyrus. Stimuli were given on the distal side of the lesion at intensities (up to 200 μA) greater than those given to non-

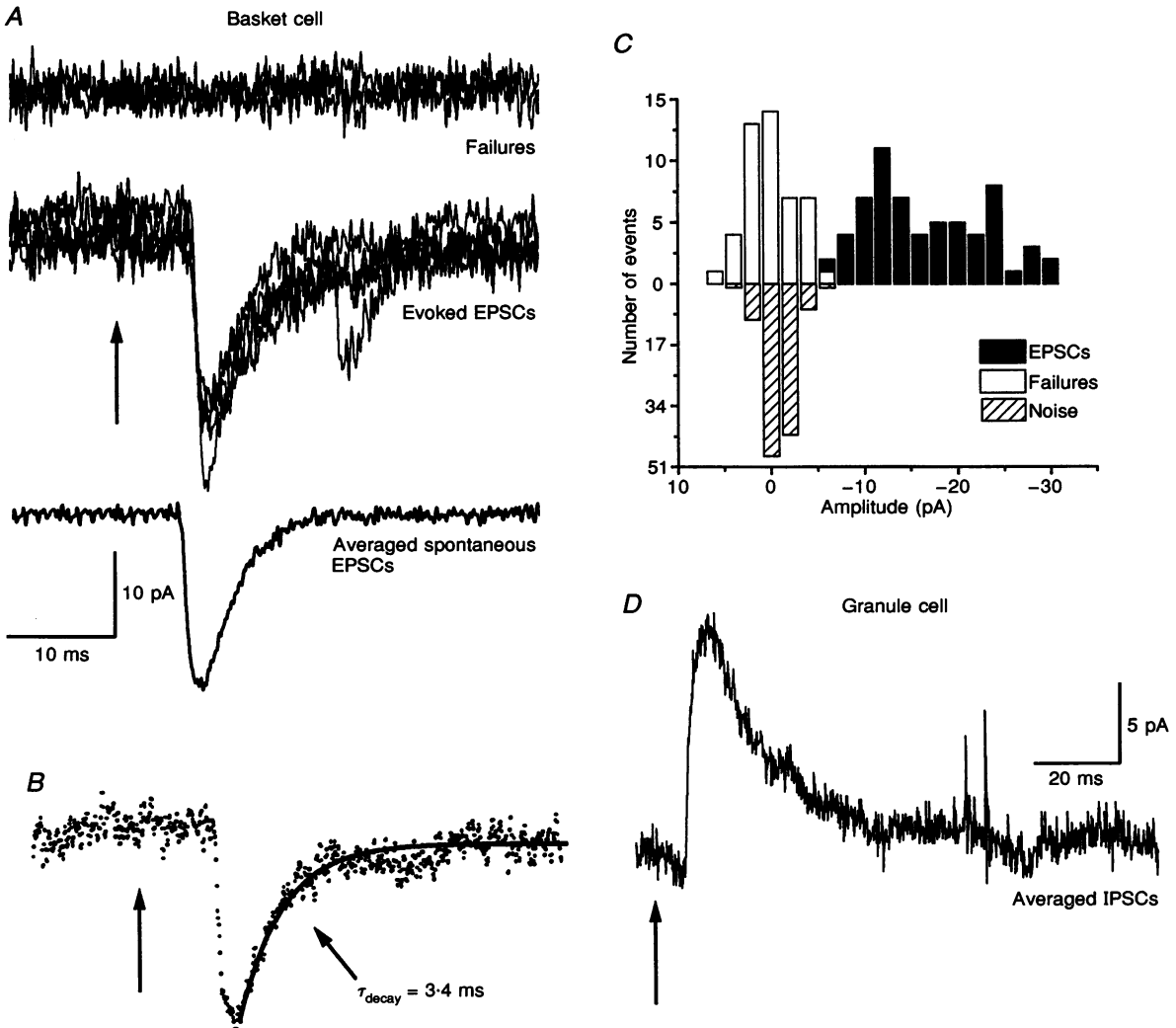

Figure 3. Basket cells receive excitatory synaptic input following CA3 pyramidal cell layer stimulation

A, CA3 pyramidal cell layer stimulation evoked EPSCs in basket cells. Some trials resulted in synaptic failures (top traces). Note that the stimulus artifact was removed from all traces by subtracting the averaged failures from each trace. Also note the similarity in time course between the evoked EPSC and a later spontaneous EPSC in one of the traces (middle) and in the average spontaneous EPSC from the same cell (lower trace). *B*, an individual evoked EPSC is shown. The kinetics for each evoked EPSC were examined; the continuous line represents the monoexponentially fitted decay time (τ_{decay}) for this EPSC. Note that spontaneous (*A*) and evoked EPSCs (*A* and *B*) have similar time courses. *C*, amplitude histogram of all evoked responses, failures (□) and EPSCs (■) in this cell. There is clear amplitude separation between EPSCs and failures. In addition to a difference in amplitude, EPSCs were distinguished from failures by their characteristic shape. Note that the amplitude distribution for the failures overlaps that of the recording noise (▨) measured just before the stimulus artifact in each trial. *D*, average response of a granule cell held at 0 mV during CA3 pyramidal cell stimulation. The latency of the response was 11 ms, suggesting that the response was probably polysynaptic. Glutamatergic transmission should be unresolvable at 0 mV since AMPA and NMDA receptor current reverses near 0 mV. Bicuculline block (not shown) of all current evoked at 0 mV confirmed that the response was GABAergic. Time of stimulation is represented by the arrows.

lesioned slices. In seven basket cells from seven slices, CA3 pyramidal layer stimulation on the distal side of the lesion never evoked monosynaptic or polysynaptic EPSCs in basket cells (e.g. Fig. 4*B* and *C*). The stimulating electrode was moved to the proximal side of the lesion in the CA3 pyramidal layer in one experiment, and EPSCs were evoked with stimulus intensities as low as 10 μA (Fig. 4*B* and *C*). These data indicated that activation of other cell types such as granule cells or hilar cells by electrical stimulation applied in the CA3 pyramidal layer was inconsequential. In six other experiments in unlesioned slices we examined the effects of stimulation of the CA3 pyramidal layer on granule cells in the presence and/or absence of 10 μM bicuculline. Neither EPSCs nor antidromic action currents were evoked by stimulation of the pyramidal cell layer (not shown). However, long latency (10–20 ms), presumably polysynaptic, IPSCs were evoked (Fig. 3*D*) when bicuculline was omitted from the bath ($n = 5$ cells). These data together suggested that an excitatory projection exists from the CA3 pyramidal layer to dentate basket cells. The lack of evoked synaptic input in basket cells in lesioned slices suggested that granule cells and other dentate neurons, even if they were activated by the stimulus, were not responsible for a significant portion of the excitatory input to the basket cells. Further, the lack of evoked EPSCs and prevalence of IPSCs in granule cells following CA3 pyramidal layer stimulation implied that a prominent functional result of CA3 pyramidal layer stimulation is granule cell inhibition. These results are most consistent with a direct excitatory projection from CA3 pyramidal cells to dentate basket cells. At present, however, we cannot eliminate completely the possibility

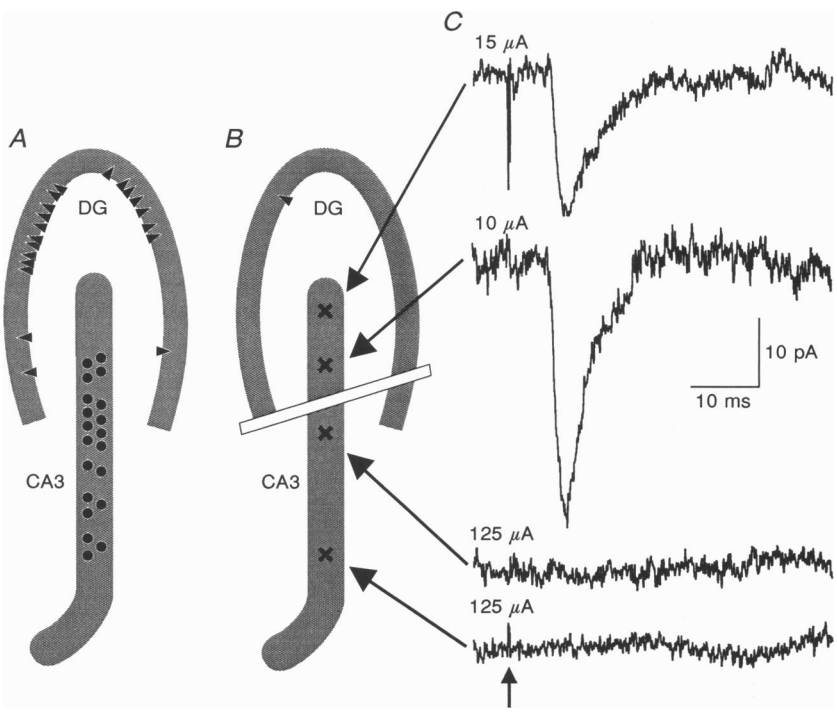

Figure 4. Activation of basket cells by stimulation in the CA3 pyramidal cell layer is eliminated by a lesion separating the dentate gyrus from CA3

A, the approximate locations of effective stimulation sites and basket cell recordings are illustrated for 20 experiments. Basket cells are represented by triangles while stimulation sites are represented by circles. CA1, not shown, is oriented to the left of the diagram. Note that the distribution of basket cells was fairly uniform throughout the dentate gyrus and that the majority of stimulation sites were outside the dentate gyrus, in CA3b or at the CA3b–c border. Stimulation of each site evoked EPSCs in the corresponding basket cell. *B* and *C*, lesioning the slice at the CA3b–c border rendered stimulation in the pyramidal layer distal to the lesion ineffective at evoking basket cell EPSCs. *B*, the location of the lesion is marked by a white rectangle. ×, stimulation site; ▲, basket cell location. *C*, the presence or absence of EPSCs in the basket cell was examined when stimuli were applied proximal (top two traces) and distal to the lesion (bottom two traces). The time of stimulation is illustrated by the arrow. Stimulus intensities are listed above each trace, which represents the average of 2–3 individual trials. Stimulation, even at very high intensities, distal to the lesion never evoked an EPSC while stimulation proximal to the lesion, with low intensity, readily evoked basket cell EPSCs. Note that the high noise level and slow EPSC kinetics are the result of deterioration of the basket cell recording as the stimulating electrode was moved to different positions. Stimulation sites were tested from most distal to most proximal.

that other unidentified fibres coursing through the CA3 pyramidal layer were activated by the stimulation.

Two observations support the idea that the stimuli were activating one or, at most, only a few pyramidal cells at a time. First, the evoked EPSC amplitudes and time courses were similar to those of spontaneously occurring EPSCs recorded in the same or other basket cells (Fig. 3*A*). The average amplitude of spontaneous EPSCs in twenty-two basket cells was $-15 \pm 2{\cdot}2$ pA, and the average rise times and decay time constants for spontaneous EPSCs were $0{\cdot}9 \pm 0{\cdot}1$ and $4{\cdot}7 \pm 0{\cdot}3$ ms, respectively. Second, the low stimulus intensity often resulted in synaptic failures (Fig. 3*A*). Although the failure rate varied between 25 and 77% in nine cells (mean, $52 \pm 9{\cdot}1$%), it did not change with time during a single experiment. The high failure rate and similar size and shape of evoked and spontaneous EPSCs argue for the stimulation of only one or a few inputs to the basket cell by any particular stimulus.

To determine whether the EPSCs were mediated by the activation of glutamate receptors, the effects of glutamate receptor antagonists were examined. The effects of the AMPA and NMDA receptor antagonists CNQX and D-APV on evoked EPSCs in two basket cells are shown in Fig. 5. When the basket cell in Fig. 5*Ba* was voltage clamped to -70 mV, 3 μM CNQX blocked nearly all the evoked current, suggesting that most of the current was carried through AMPA-type glutamate receptors. In the basket cell shown in Fig. 5*A*, 50 μM D-APV altered the time course of the EPSCs recorded at -70 mV (control *vs.* D-APV treated: rise time, 1·6 *vs.* 1·2 ms; decay time constant, 6·3 *vs.* 3·8 ms; amplitude, -27 *vs.* -32 pA; $n = 25$–30 EPSCs) suggesting that some of the current was mediated by NMDA receptors. Depolarizing the basket cell to +40 mV to relieve the magnesium block revealed a larger contribution of NMDA receptor-mediated current (Fig. 5*A* and *Bb*). When the basket cell in Fig. 5*A* was depolarized to +40 mV, the rise time of the evoked EPSCs was considerably slower than that at -70 mV (at +40 mV, 3·5 ms), and the decay time constant at +40 mV was best fitted by the sum of two exponentials (54 and 8·2 ms). The addition of 50 μM D-APV blocked the slower phase of the EPSCs (Fig. 5*A*). The addition of 3 μM CNQX to the basket cell in Fig. 5*Bb* slowed the time course of the EPSCs at +40 mV (control *vs.* CNQX treated: rise time, 4·4 *vs.*

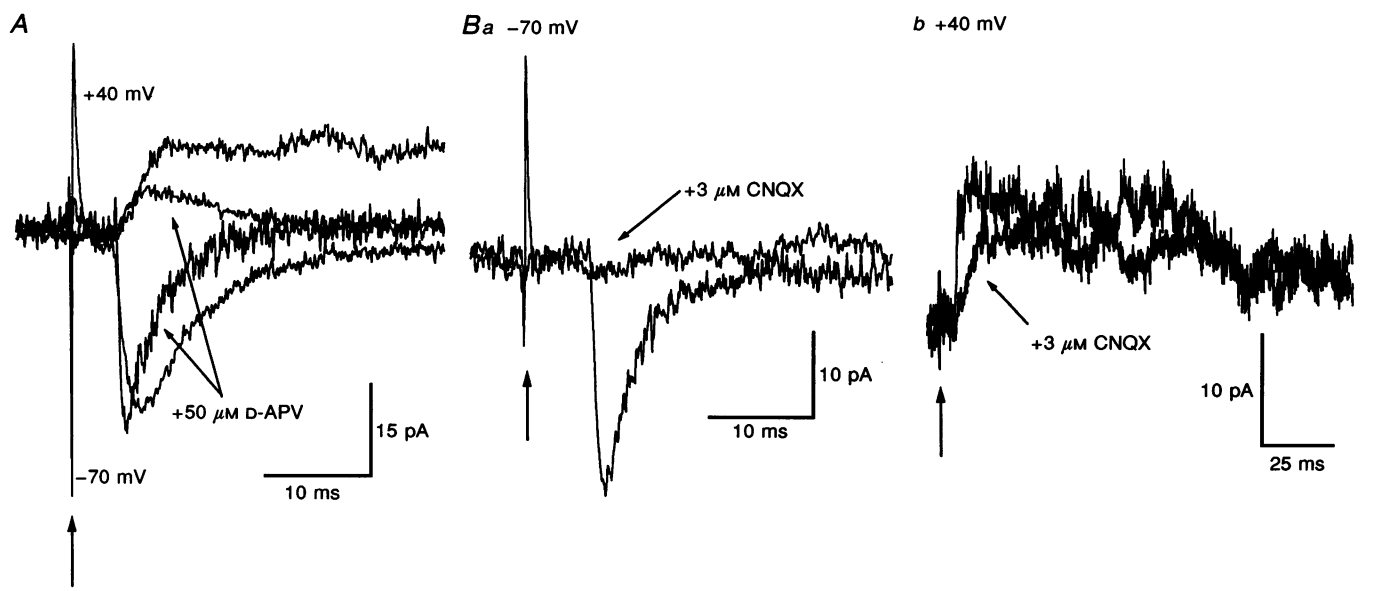

Figure 5. Basket cell EPSCs evoked by CA3 pyramidal cell layer stimulation are mediated by both AMPA and NMDA receptors

Recordings from two different basket cells (*A* and *B*) during CA3 pyramidal cell layer stimulation. *A*, the basket cell was voltage clamped to -70 mV and +40 mV in the absence and presence of the NMDA receptor antagonist D-APV. D-APV blocked a small fraction of the current at -70 mV but had a much more pronounced effect on the current at +40 mV. The EPSC rise time and decay time at -70 mV were faster in the presence of 50 μM D-APV. The rise time decreased from 1·6 to 1·2 ms, and the decay time constant decreased from 6·3 to 3·8 ms. The kinetics of the EPSCs at +40 mV also changed in D-APV. The rise time decreased from 3·5 to 1·7 ms in D-APV. The decay phase, fitted by two exponentials (54 and 8·2 ms) in control conditions, was well fitted by a single exponential (7·3 ms) in D-APV. *B*, the basket cell was voltage clamped to either -70 (*Ba*) or +40 mV (*Bb*) in the presence or absence of the AMPA receptor antagonist CNQX. CNQX blocked nearly all the current at -70 mV (*Ba*) and had a lesser effect on the current at +40 mV (*Bb*). The rise time of the EPSCs at +40 mV was slowed from 4·4 to 8·3 ms. The decay time, fitted by two exponentials in control conditions (35 and 20 ms), could be fitted by a single, longer exponential in CNQX (84 ms). Arrows mark the stimulus artifact.

8·3 ms; decay time constant, 35 and 20 ms *vs.* 84 ms) and reduced the amplitude slightly. The subsequent addition of 50 μM D-APV to the cell eliminated all current (not shown).

For five basket cells depolarized to +40 mV the average EPSC rise time was 4·3 ± 0·2 ms, the double exponential decay time constants were 8·9 ± 2·7 and 98 ± 11 ms, and the amplitude was 13 ± 2·8 pA. In all five cells CNQX and D-APV blocked a fraction of the current at both hyperpolarized and depolarized potentials, and the simultaneous addition of CNQX and D-APV abolished all current, suggesting that NMDA and AMPA receptors coexist at these synapses and mediate CA3 pyramidal cell evoked EPSCs.

Monosynaptic EPSCs and polysynaptic GABAergic control of the pathway

Monosynaptic and polysynaptic EPSCs can be distinguished based on their different response to reducing extracellular calcium. The latency of polysynaptic EPSCs should increase as extracellular calcium is decreased because spikes in the intervening neuron would be triggered later on a more slowly rising EPSP. The latency of monosynaptic EPSCs, on the other hand, should be unaffected by decreased calcium since only one synapse is involved in the pathway. As the calcium concentration decreases further, transmission along polysynaptic pathways will be completely interrupted followed by the

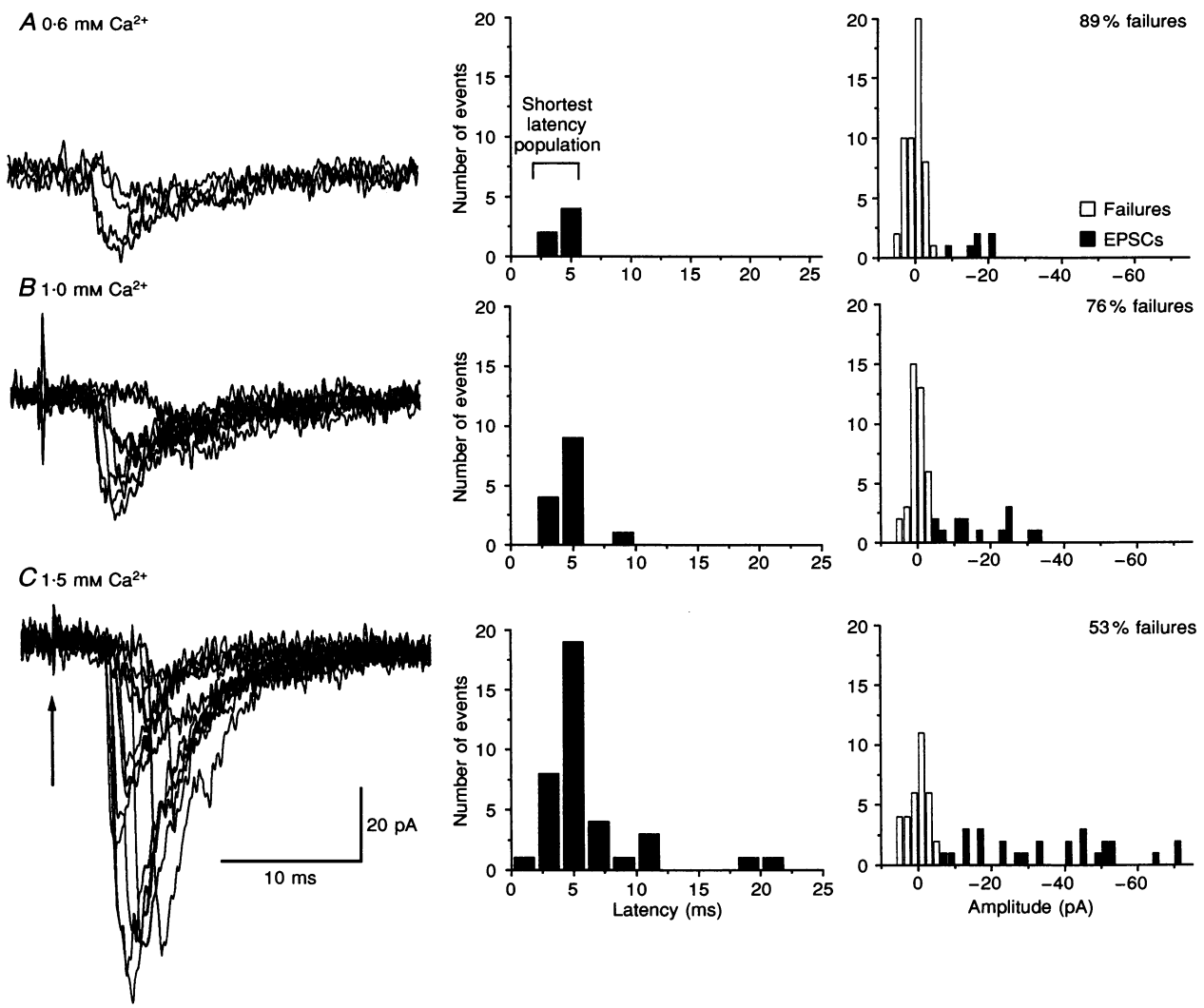

Figure 6. CA3 pyramidal cell stimulation evokes monosynaptic EPSCs in basket cells

Basket cell EPSCs were examined in decreasing extracellular calcium concentrations during CA3 pyramidal cell layer stimulation. EPSCs evoked in 0·6 mM (*A*), 1·0 mM (*B*), and 1·5 mM (*C*) extracellular calcium are illustrated in the left panels. The arrow shown in *C* is the time of the stimulus artifact and refers to *A* and *B* also. Failures increased and EPSC amplitudes decreased as extracellular calcium decreased (right panels). A short latency EPSC population persisted in 0·6 mM calcium (*A*, middle panel), suggesting that they were monosynaptically mediated. The failure rate for short latency EPSCs in this basket cell increased from 53 to 89%, and the EPSC amplitude (right panels) decreased as the calcium concentration was dropped from 1·5 (*C*) to 0·6 mM (*A*).

interruption of the monosynaptic pathways as calcium decreases even more. Utilizing this difference in sensitivity to extracellular calcium between polysynaptic and monosynaptic pathways, we compared electrically evoked EPSCs in basket cells in normal 1·5 mM extracellular calcium with EPSCs in 0·6 mM extracellular calcium to determine whether the input to basket cells from CA3 was monosynaptically or polysynaptically mediated.

Our results revealed that the evoked EPSCs were both monosynaptically and polysynaptically mediated. Electrical stimulation of the CA3 pyramidal cell layer in normal 1·5 mM calcium-evoked EPSCs in basket cells that varied in latency. Example EPSCs recorded in the absence of bicuculline in each of three calcium concentrations are shown in Fig. 6 (left panels). The variability in EPSC latency is demonstrated in the latency–frequency histogram in Fig. 6*C* (middle panel). When calcium was reduced from 1·5 to 1·0 mM and finally 0·6 mM, the shortest latency EPSCs (denoted by the bracket in Fig. 6*A*, middle panel) persisted with no increase in latency (Fig. 6, middle panels), indicating that those EPSCs were monosynaptically mediated. The amplitude of the shortest latency EPSCs in this basket cell decreased from $-34 \pm 4{\cdot}2$ pA ($n = 27$ EPSCs) in 1·5 mM calcium to $-17 \pm 1{\cdot}9$ pA ($n = 6$ EPSCs) in 0·6 mM calcium. The EPSC amplitude distributions shifted to the left as the calcium concentration decreased (Fig. 6, right panels). The decrease in EPSC amplitude and increase in percentage of failures (53% in 1·5 mM calcium to 89% in 0·6 mM calcium) with no change in latency in decreased calcium is consistent with decreased probability of release at monosynaptic synapses. Similar results were obtained in two other basket cells.

Some EPSCs with long and variable latency were probably polysynaptically mediated since they disappeared in low calcium conditions (Fig. 6). When 10 μM bicuculline was applied to the slice to reduce GABAergic inhibition, a greater polysynaptic input became apparent. In the basket cell shown in Fig. 7 bicuculline revealed evoked polysynaptic EPSCs with latencies as long as 70 ms. The short latency and longer latency EPSCs examined in all

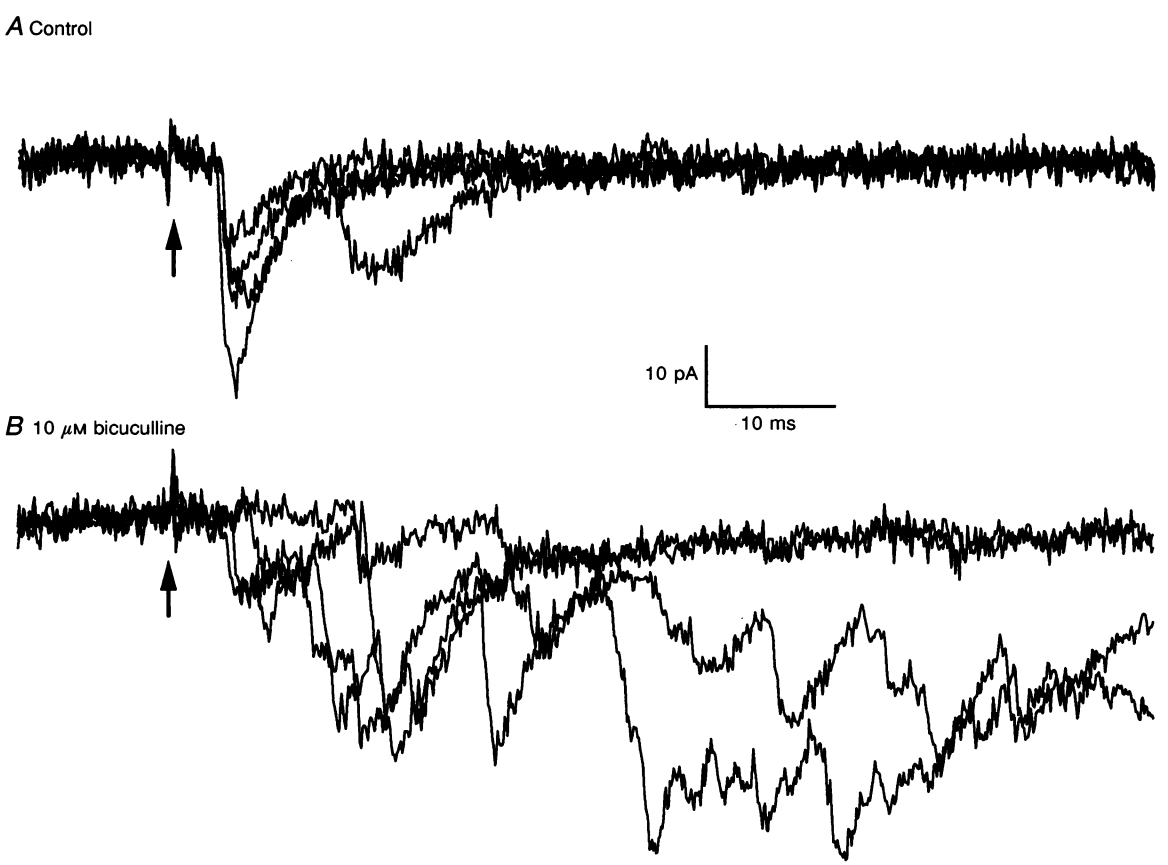

Figure 7. Polysynaptic EPSCs are more apparent in disinhibited slices

Although some longer latency EPSCs were evoked by CA3 pyramidal cell layer stimulation in control ACSF (*A*), a larger population of polysynaptic EPSCs was revealed when the $GABA_A$ antagonist bicuculline was added to the slice (*B*). These data suggest that the CA3 pyramidal cell–basket cell polysynaptic pathway is normally under strong inhibitory control and that the pathway may be more physiologically significant when inhibition in the slice is disrupted. The stimulus artifact is indicated by the arrows.

basket cells were similar in size and shape (at −70 mV, longer latency EPSC rise time, 0·7 ± 0·1 ms; decay time constant, 3·7 ± 0·2 ms; amplitude, −13 ± 0·6 pA; $n = 6$ cells, $P > 0·3$ for all measurements *vs.* shortest latency EPSCs), suggesting that similar synapses may have been utilized for both monosynaptic and polysynaptic pathways. Whatever the presynaptic source of the EPSCs, this extensive polysynaptic pathway would strongly activate basket cells when tonic inhibition of the pathway was reduced, effectively increasing the inhibitory input to granule cells.

Synchronous firing of CA3 pyramidal cells activates basket cells

Using single unit extracellular recordings of spontaneously occurring action potentials in CA3 pyramidal cells together with whole-cell recordings of synaptic currents in basket cells, we sought to confirm that action potentials arising in CA3 pyramidal cells cause EPSCs in basket cells and to determine which CA3 pyramidal cell firing patterns most effectively activate basket cells. In recordings from 103 pyramidal cells paired with 11 basket cells in 11 slices only two connections were identified, both polysynaptic. One

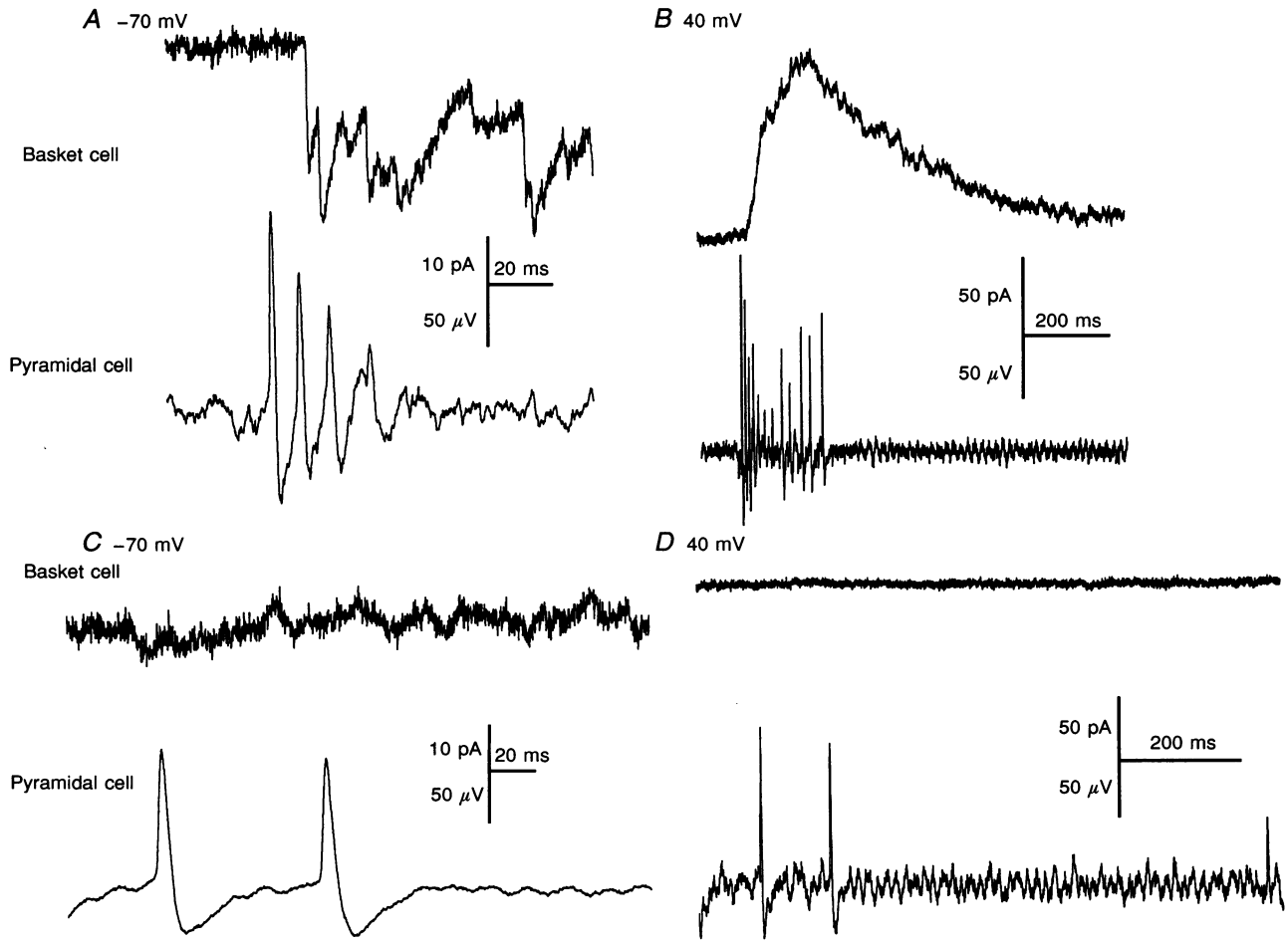

Figure 8. CA3 pyramidal cell action potential bursts evoke EPSCs in basket cells

A voltage-clamped basket cell (top trace in each panel) was examined simultaneously with an extracellularly recorded CA3 pyramidal cell (bottom trace). *A* and *B*, clusters of EPSCs appeared in the basket cell following a burst of action potentials in the CA3 pyramidal cell when the basket cell was voltage clamped to −70 (*A*) and +40 mV (*B*). Note that the time scale in *B* is ten-fold larger than that in *A* to accommodate the temporal summation of EPSCs at +40 mV. Of the 15 bursts that occurred in this CA3 pyramidal cell, all were followed by a cluster of EPSCs in the basket cell. Note that the first EPSC in the cluster (*A*, top trace) did not occur until ~12 ms after the peak of the first CA3 pyramidal cell action potential (*A*, bottom trace) and that the 4 or 5 action potentials in the CA3 pyramidal cell evoked about 18 basket cell EPSCs (not all EPSCs are shown) suggesting that the EPSCs were polysynaptically mediated. *C* and *D*, single CA3 pyramidal cell action potentials did not evoke EPSCs in the basket cell clamped to −70 (*C*) or +40 mV (*D*). No reproducible EPSCs were observed in this basket cell following 3642 single action potentials.

pair is shown in Fig. 8. In each panel in Fig. 8 the extracellular recording from the CA3 pyramidal cell is in the lower trace, and the whole-cell recording from the basket cell is in the upper trace. A burst of action potentials in the CA3 pyramidal cell elicited a burst of EPSCs in the basket cell (Fig. 8*A*) that summed temporally to a long-lasting synaptic current when the basket cell was voltage clamped to +40 mV (Fig. 8*B*). The reversal potential and kinetics of the EPSCs were similar to those of electrically evoked EPSCs in other cells, suggesting that the EPSCs may have been mediated by similar synapses. In the pair shown in Fig. 8*A* the delay from the peak of the first action potential to the foot of the first EPSC was about 12 ms, and the four or five action potentials in the CA3 pyramidal cell evoked about eighteen EPSCs in the basket cell suggesting that the EPSCs were mediated polysynaptically. Of the fifteen presynaptic spike bursts examined in this cell, all were followed by clusters of EPSCs.

Interestingly, single action potentials in the same CA3 pyramidal cell appeared incapable of activating the pathway (Fig. 8*C* and *D*). Since the spontaneous EPSC frequency in all basket cells was fairly high (5·3 ± 0·4 Hz, $n = 12$ cells) and electrical stimulation resulted in failures in over 50% of the trials as discussed previously, casual inspection would be insufficient to rule out EPSCs driven from single spikes. Therefore, the number of EPSCs occurring 8 ms before and after twenty-five randomly chosen pyramidal cell action potentials was counted for each pair. An 8 ms window represented a liberal estimate of the maximum latency for monosynaptic EPSCs based on electrical stimulation experiments. In the basket cell shown in Fig. 8 no EPSCs occurred in the 8 ms before or after the twenty-five randomly chosen pyramidal cell action potentials. Indeed, when the entire data record for the cell pair in Fig. 8 was visually inspected, there was no clear difference between the likelihood of a basket cell EPSC preceding or following 3642 single pyramidal cell action potentials, and the latencies of the EPSCs that did follow the action potentials were dissimilar, ranging from 2 to 7 ms.

In all 103 pairs a substantial difference was never found between the number of EPSCs occurring 8 ms before (7·7 ± 1·3% of the trials) or after (9·5 ± 1·4% of the trials) CA3 pyramidal cell action potentials. Although the likelihood of an EPSC occurring in the 8 ms after compared to 8 ms before the spike was on the border of statistical significance ($P = 0·049$ by paired t test), the EPSCs in any given cell were much less frequent than predicted by electrical stimulation, had latencies that varied by several milliseconds, and could not be distinguished from spontaneously occurring events. Monosynaptic connections also were not found in eighty-six granule cell–basket cell pairs although basket cell EPSCs were readily evoked by electrical stimulation of the granule cell layer (Kneisler & Dingledine, 1995) and granule cell synapses onto basket cells have been demonstrated previously (Ribak & Peterson, 1991). These data suggest that either monosynaptic connections between the CA3 pyramidal cells and basket cells are sparse or that the average failure rate of the monosynaptic pathway (~50%) was underestimated and precluded distinction of monosynaptic EPSCs from spontaneous EPSCs. Our inability to detect connected CA3 pyramidal and basket cells may have resulted from some combination of low reliability *and* low connectivity. The apparent inability of single CA3 pyramidal cell action potentials to evoke basket cell EPSCs suggested that a burst of CA3 pyramidal cell spikes may be required in order for the pathway to be physiologically relevant.

Elevation of the extracellular potassium concentration causes CA3 pyramidal cells to fire synchronously in bursts (Rutecki, Lebeda & Johnston, 1985; Yaari, Konnerth & Heinemann, 1986; Korn, Giacchino, Chamberlin & Dingledine, 1987). These interictal events arise spontaneously in the CA3b and CA3c subfields and involve synchronous action potential firing in many CA3 pyramidal cells and some hilar neurons. Granule cells, however, are not involved in potassium-induced interictal burst firing unless the extracellular potassium exceeds 12 mM or the extracellular calcium concentration is lowered to 0·9 mM (Patrylo, Schweitzer & Dudek, 1994). We examined the effect of raised potassium on basket cells since it appeared from the paired recordings that basket cells would be strongly activated by CA3 pyramidal cell burst firing.

Due to the young age of the rats used for our experiments, CA3 pyramidal cell population bursts in elevated potassium occurred regularly but were less synchronized than those commonly observed in adult rats. Nevertheless, raising extracellular potassium from 3·5 to 8·5 mM resulted in spontaneous bursts of action potentials (Fig. 9*A*) and periodic barrages of EPSCs (Fig. 9*C*) in basket cells that occurred with a similar frequency as the CA3 pyramidal cell bursts. The basket cell shown in Fig. 9*Cb* received a cluster of EPSCs every 4·2 ± 0·2 s that lasted 200 ± 20 ms. The clusters of EPSCs resulted in action potential firing in the basket cells studied under current clamp.

The spontaneous EPSC clusters that appeared in raised potassium in the basket cell in Fig. 9*C* were nearly abolished by the glutamate receptor antagonists CNQX and D-APV. Although this finding did not indicate that the excitatory synapses on basket cells themselves were mediated by glutamate, it did demonstrate the involvement of AMPA and NMDA receptors at some synapses in the pathway. The EPSCs recorded in all ten basket cells in 8·5 mM potassium were similar to those occurring spontaneously in 3·5 mM potassium, those evoked by CA3 pyramidal cell layer electrical stimulation, and those evoked by action potential bursts in single CA3 pyramidal cells except that the amplitudes of the EPSCs within the clusters recorded in raised potassium were larger than

EPSCs observed in normal potassium. In 8·5 mM extracellular potassium the average basket cell EPSC rise time for ten cells was 0·6 ± 0·1 ms, the decay time constant was 2·7 ± 0·1 ms, and the amplitude was −22 ± 1·1 pA. We were unable to determine the temporal correlation between CA3 pyramidal cell firing and basket cell excitation since the start of CA3 pyramidal cell bursting was not as sharply defined as in adult.

Though we could not rule out the possibility that the potassium-induced input to basket cells was derived from a source other than CA3 pyramidal cells, it appeared unlikely that the input was the result of granule cell activity. Whole-cell recordings from granule cells were made to determine whether granule cells fired action potentials in elevated potassium and to determine whether elevated potassium evoked excitatory or inhibitory synaptic currents in granule cells. The granule cell shown in Fig. 9*B* depolarized 15 mV in 8·5 mM potassium but never fired an action potential. In all three granule cells examined, no action potentials were evoked although the membrane potential depolarized from 4 to 20 mV (mean, 13 ± 4·7 mV) in 8·5 mM potassium.

Changes in spontaneous EPSC and IPSC frequency in four granule cells in raised potassium were also examined. The granule cell in Fig. 10 was voltage clamped to −50 or 0 mV to determine the frequency of EPSCs and IPSCs, respectively, in 3·5 and 8·5 mM potassium. There was no increase in EPSC frequency (0·36 Hz in 3·5 mM KCl; 0·37 Hz in 8·5 mM KCl) or amplitude (−2·6 *vs.* −3·0 pA), but IPSC frequency increased from 2·0 to 7·1 Hz as shown in Fig. 10*B*. The currents recorded at 0 mV were GABAergic IPSCs since they were blocked by 10 μM bicuculline (Fig. 10*B*). The increased IPSC frequency was probably the result of heightened interneuron excitability.

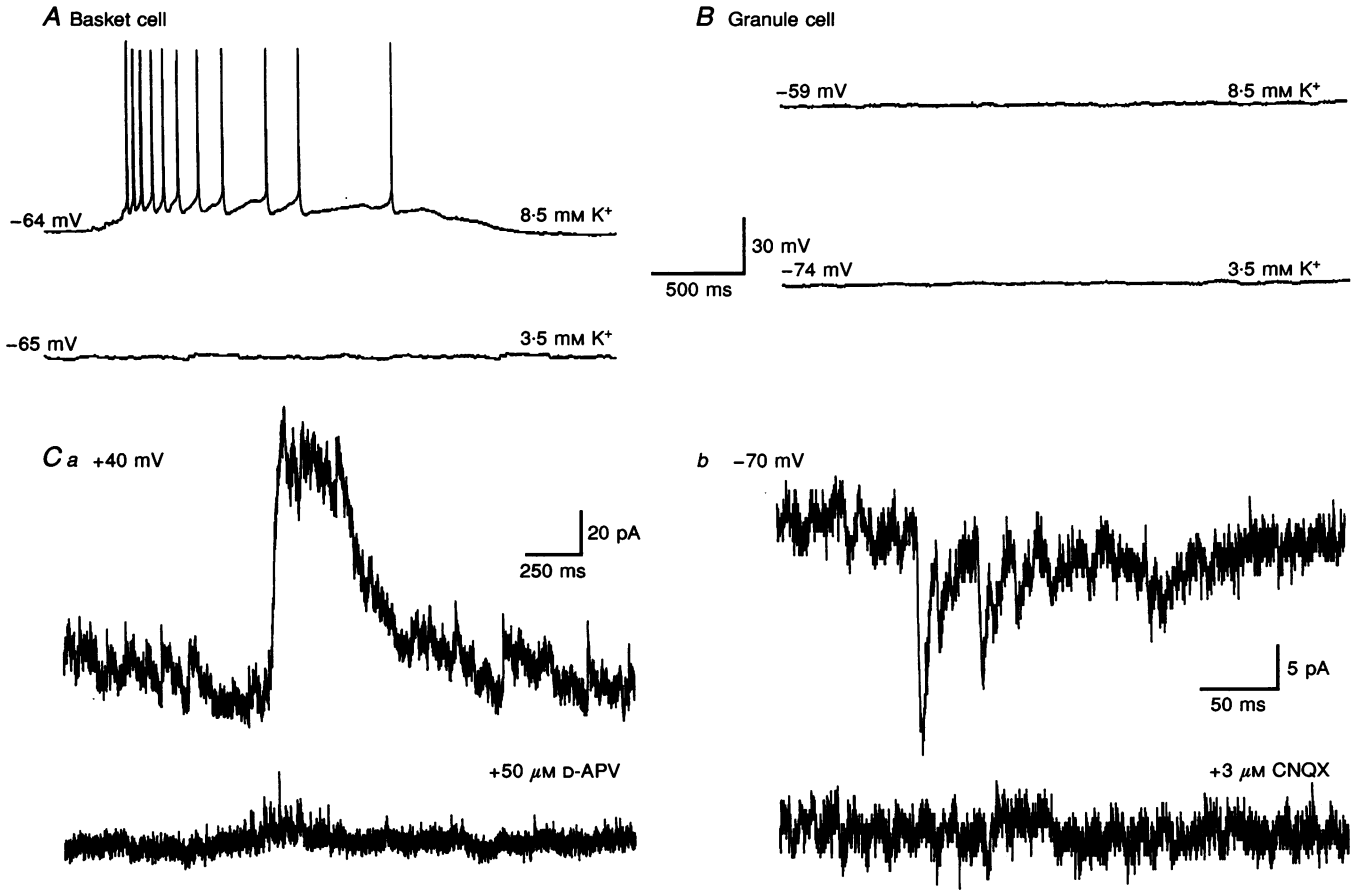

Figure 9. Elevated potassium elicits clusters of EPSCs in basket cells resulting in action potential bursts

A, in 8·5 mM potassium this basket cell fired spontaneous action potentials in bursts with the same frequency (0·33 Hz) as CA3 pyramidal cell bursts. *B*, granule cell in 3·5 and 8·5 mM extracellular potassium. Though the granule cell depolarized in 8·5 mM potassium, it never fired an action potential suggesting that the increased excitability of basket cells was unlikely to be due to granule cell firing. *C*, the basket cell action potentials were synaptically driven. This voltage-clamped basket cell received clusters of EPSCs that occurred with a similar frequency as CA3 pyramidal cell bursts. The EPSCs were partially blocked by the NMDA and AMPA receptor antagonists D-APV (*Ca*) and CNQX (*Cb*).

In all four granule cells examined, the EPSC frequency (0·4 ± 0·1 Hz in normal potassium *vs.* 0·5 ± 0·1 Hz in 8·5 mM potassium, $P > 0·7$) and amplitude (6·3 ± 1·1 pA *vs.* 4·0 ± 0·2 pA, $P > 0·2$) were unchanged in raised potassium while the frequency of bicuculline-sensitive IPSCs increased three-fold, from 1·8 ± 0·1 to 5·3 ± 0·6 Hz ($P < 0·05$).

Paired-pulse facilitation of the excitatory input

We investigated whether the CA3 pyramidal cell–basket cell synapse showed short term plasticity to examine further and reinforce the notion that the pathway was better activated by a short train of action potentials than by a single action potential. Paired-pulse facilitation is

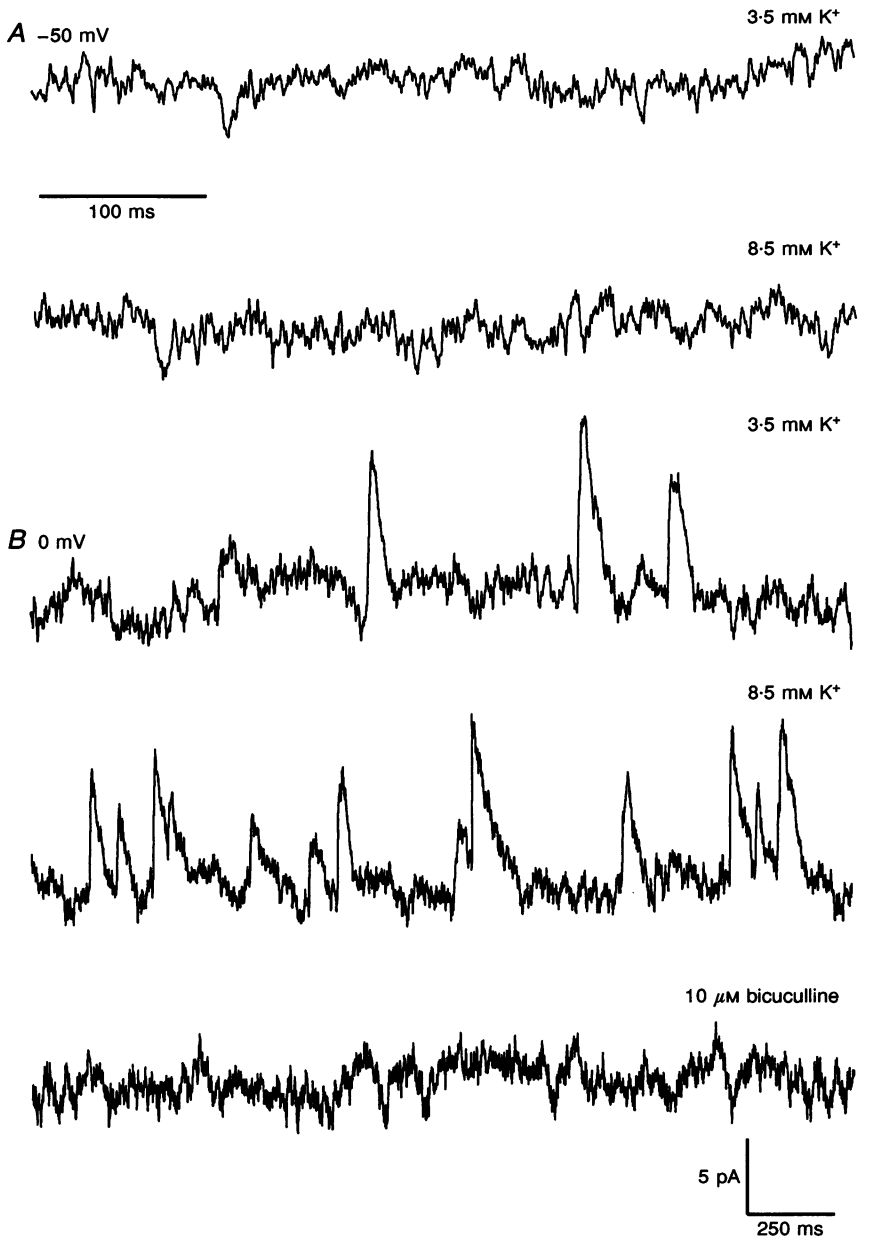

Figure 10. Granule cells receive increased inhibitory input but not increased excitatory input in elevated potassium

This granule cell was voltage clamped to either −50 or 0 mV in both 3·5 and 8·5 mM potassium. At −50 mV, near the reversal potential for chloride, net current through GABA receptors should be negligible. At 0 mV, near the reversal potential for monovalent cations, net current through glutamate receptors should be immeasurable. *A*, unlike that seen in basket cells, no increase in EPSC frequency was seen in this granule cell in 8·5 mM potassium (0·36 Hz in 3·5 mM potassium (upper trace) and 0·37 Hz in 8·5 mM potassium (lower trace)). *B*, IPSC frequency, however, increased from 2·0 Hz (upper trace) in 3·5 mM potassium to 7·1 Hz (middle trace) in 8·5 mM potassium. The synaptic currents at 0 mV were $GABA_A$ receptor mediated since they were completely blocked by 10 μM bicuculline (lower trace).

defined as an increase in the amplitude of the second response with paired stimulation and at other synapses is thought to be due to an increased probability of release (Zucker, 1989). We showed that this synapse was capable of paired-pulse facilitation and determined a probable mechanism.

Figure 11*D* shows typical results from a basket cell following pairs of minimal intensity CA3 pyramidal layer stimulation. In this cell seventy-nine stimulus pairs were delivered 40 ms apart, and the failure rates and amplitudes of the EPSCs were determined. Evoked EPSCs in this basket cell were more likely following the second stimulus

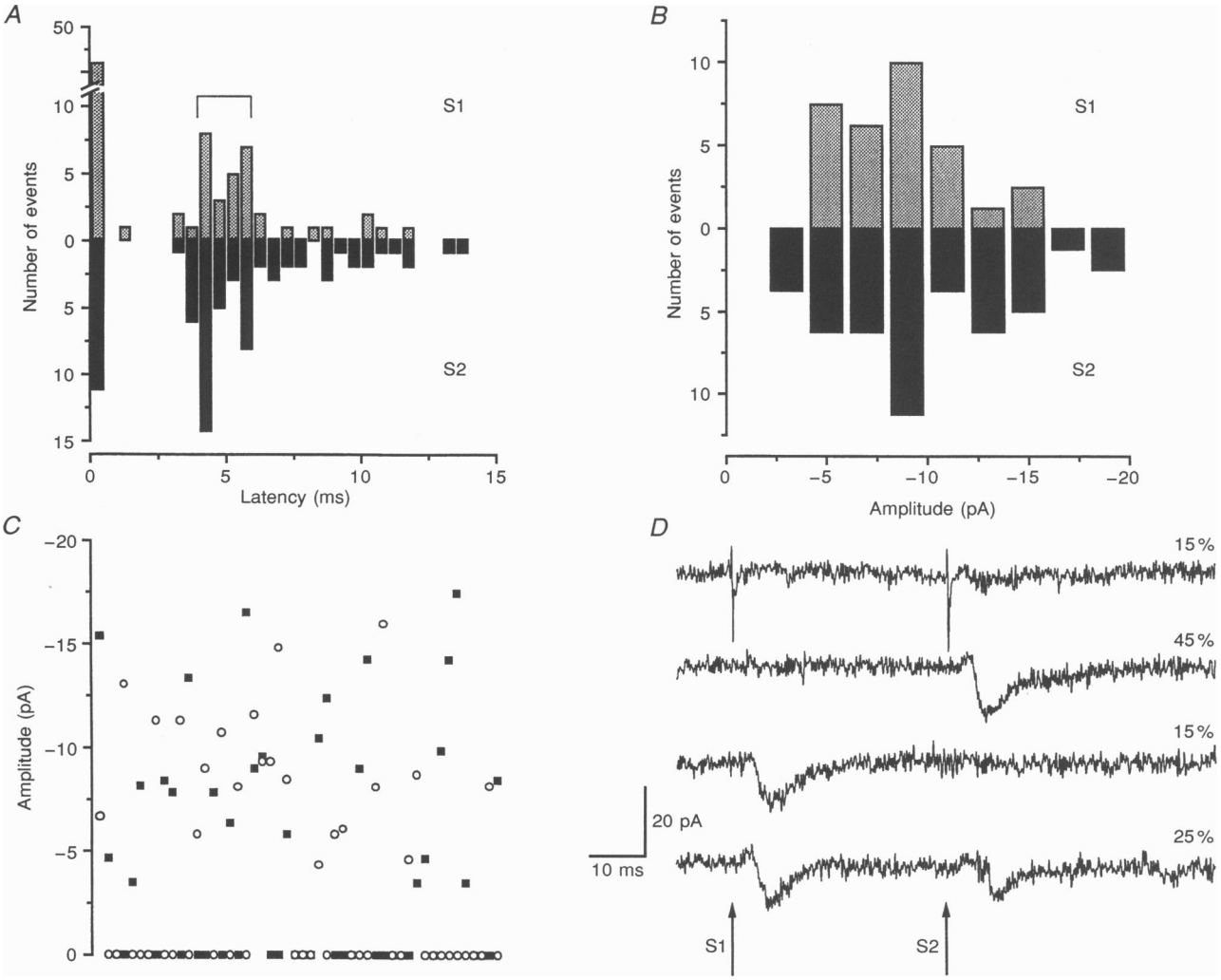

Figure 11. Paired-pulse facilitation of the CA3 pyramidal layer input

Two stimuli given within 40 ms of each other resulted in four responses from this basket cell voltage clamped to −70 mV. *A*, the histograms represent the latency of EPSCs following the first stimulus, S1 (▨) and the second stimulus, S2 (■). The latency of all EPSCs evoked using the paired-pulse stimulation paradigm was distributed over about 9 ms. To examine a single or a few release sites we chose the population of EPSCs corresponding to the shortest latency (bracketed). This population was used for further analysis. The bars at 0 ms represent failures. Note that the number of failures decreased from 42 following S1 to 11 following S2 in 79 trials. *B*, the amplitude distributions of the S1 and S2 EPSCs in this cell were similar, suggesting that potentiation of the synapse did not involve an increase in the amplitude of individual EPSCs. *C*, EPSC amplitude was also unchanged over the course of the experiment confirming that neither response rundown nor any long term potentiation or depression of the synapse developed. Failures are represented by the symbols at 0 pA. The number of failures following S1 (○) and S2 (■) did not change over the course of the experiment. *D*, representative traces. The most frequent response (45% of the time) was an S1 failure and an S2 EPSC. An S2 EPSC occurred 70% of the time while an S1 EPSC occurred in only 40% of the trials. An S2 EPSC was as likely to follow an S1 EPSC (63%) as an S1 failure (75%) suggesting that prior release history did not affect release probability.

(70%) than following the first (40%), consistent with an increased probability of release following the second stimulus (Fig. 11*D*). An EPSC triggered by the second stimulus (S2) following an EPSC evoked by the first stimulus (S1) occurred with similar probability (63%) as an S2 EPSC following an S1 failure (75%). Of the nine basket cells in which paired stimuli were applied, failures decreased from 48 ± 9·2% following S1 to 33 ± 11% following S2.

The latency of the evoked EPSCs in the basket cell shown in Fig. 11 varied considerably, implying that several pathways, both monosynaptic and polysynaptic, may have been activated. Latency histograms for S1 and S2 EPSCs in this basket cell are shown in Fig. 11*A*. To examine paired-pulse facilitation for one or, at most, only a few synaptic inputs, the EPSCs with the shortest latencies (denoted by the bracket in Fig. 11*A*) were selected for further analysis. The latency (Fig. 11*A*) and amplitude distributions (Fig. 11*B*) and similar kinetics (not shown) of the selected EPSCs suggested that they arose from the activation of a similar population of synapses.

Although the failure rates of the early latency EPSCs following the first and second stimuli differed in the basket cell considered in Fig. 11, the mean EPSC amplitudes did not (Fig. 11*B*). The mean amplitude of the S1 EPSCs (−8·5 ± 0·6 pA, $n = 26$ EPSCs) was not significantly different from the mean amplitude of the S2 EPSCs (−9·8 ± 0·7 pA, $n = 37$ EPSCs, $P > 0{\cdot}15$). In addition, the amplitude of the EPSCs following both stimuli was unchanged over the course of the experiment (Fig. 11*C*), suggesting that neither response rundown nor any slowly developing long term potentiation or depression developed during the experiment. When failures were considered in the mean amplitude calculations in the cell shown in Fig. 11, however, mean amplitudes of the S1 and S2 EPSCs were significantly different (−2·8 ± 0·5 *vs.* −4·6 ± 0·6 pA, $n = 79$ paired stimuli, $P < 0{\cdot}05$). This was expected since there were more failures following the first stimulus.

Data for paired stimulation of all nine basket cells examined are summarized in Fig. 12. As mentioned above, within any experiment only EPSCs with similar latencies were compared (Fig. 12*C*). The failure rate (Fig. 12*A*) for those EPSCs with similar latencies decreased from 72 ± 5·2% following S1 to 53 ± 5·9% following S2 ($n = 9$, $P < 0{\cdot}001$ by paired t test). In each basket cell tested, the mean amplitude of the EPSCs evoked by the first stimulus

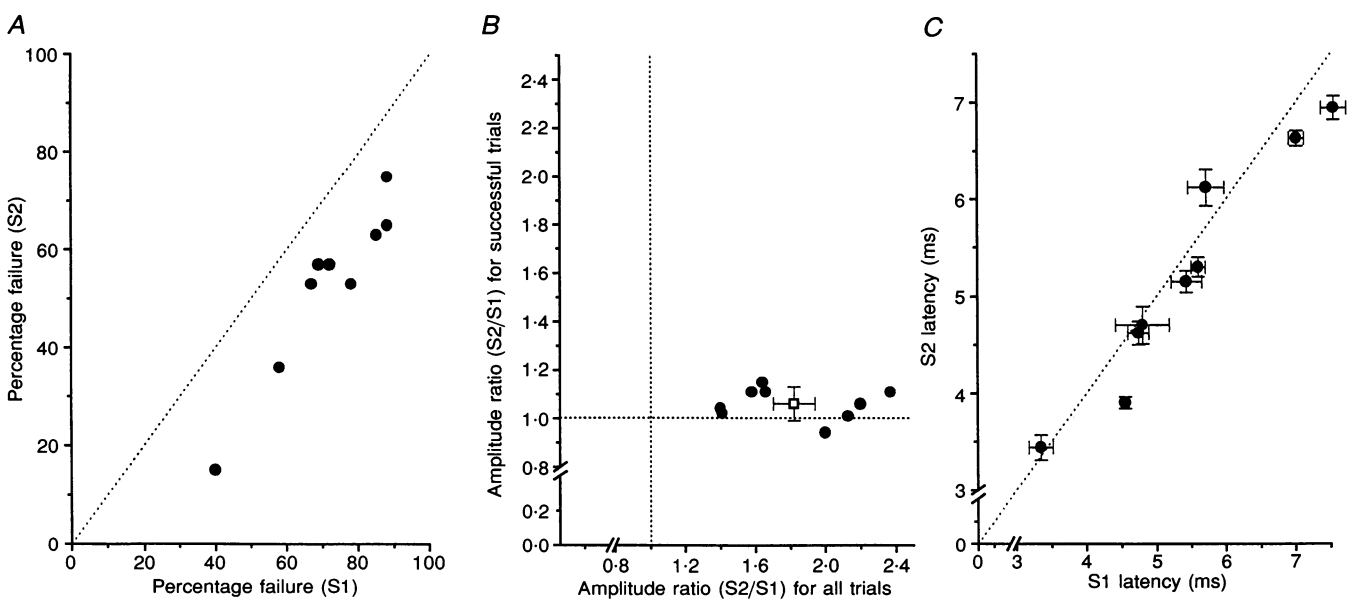

Figure 12. Paired-pulse facilitation results from a decrease in failure rate

A, the failure rate following S2 was always less than that following S1 suggesting that the probability of release of the synapse was increased. Responses along the diagonal dotted line would indicate no change in failure rate. Each filled circle represents data from a different neuron subjected to at least 67 paired stimuli. *B*, the amplitude of the EPSCs did not change following S1 and S2 (y axis, S2/S1 ≈ 1·0). If the amplitudes of all responses (failures and EPSCs) were considered in the amplitude average, an ~1·8 fold potentiation of the S2 response could be observed (x axis). Points on the horizontal line would indicate no change in S1 and S2 EPSC amplitude while points on the vertical line would indicate no net facilitation (no change in EPSC amplitude or failure rate following S1 and S2). The open box shows the mean ± S.E.M. S2/S1 ratio for all 9 cells. *C*, the latency of the EPSCs following S1 and S2 was unchanged suggesting that the same or similar synapses were involved. Points on the diagonal line indicate no difference between the latency of S1 EPSCs and S2 EPSCs.

was no different from the mean amplitude of the EPSCs evoked by the second stimulus ($-15 \pm 0{\cdot}6$ *vs.* $-16 \pm 0{\cdot}7$ pA, $n = 9$ basket cells, $P > 0{\cdot}2$). If failures were included in the analysis, however, the mean amplitude of the EPSCs was larger following the second stimulus ($-5{\cdot}7 \pm 0{\cdot}4$ *vs.* $-9{\cdot}6 \pm 0{\cdot}6$ pA, $n = 9$ basket cells, $P < 0{\cdot}01$). As shown in Fig. 12*B*, when the ratio of the amplitudes of the S1 and S2 EPSCs was compared with the S2/S1 amplitude ratio for all trials (failures and successes), it was clear that, although individual EPSCs were not potentiated (S2/S1 ≈ 1, y axis) the average response was potentiated (S2/S1 $\approx 1{\cdot}8$, x axis).

These data demonstrate that the CA3 pyramidal cell–basket cell pathway was capable of paired-pulse facilitation and that the mechanism of this facilitation was increased probability of release. We cannot exclude a more efficient activation of the presynaptic element by the second stimulus, but since our stimuli were given every 3 s rather than in long trains used by others to demonstrate threshold reduction (e.g. Poolos, Mauk & Kocsis, 1987; McNaughton, Shen, Rao, Foster & Barnes, 1994), this explanation is unlikely to account for the observation. Indeed, using stimulation paradigms similar to the one employed in this study, it has been shown that although a small fraction of failures can be explained by failure to activate the presynaptic cell or conduction failure, synaptic failures result primarily from a low probability of release from the synapse (Allen & Stevens, 1994). These results reinforce the conclusion that this pathway is better activated by a short train of action potentials than a single input.

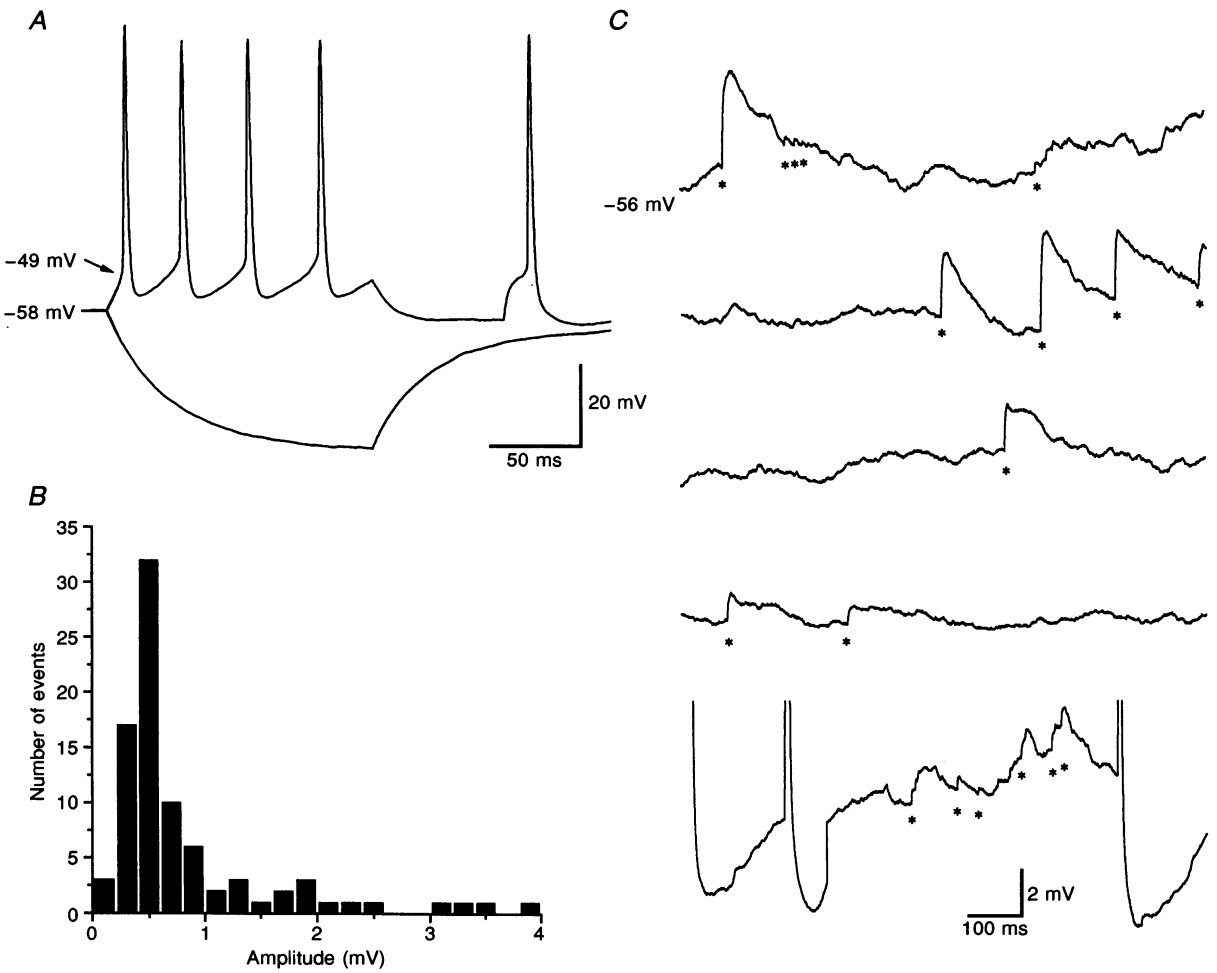

Figure 13. Number of inputs required for basket cell activation

A, in this basket cell the threshold for action potential generation was about +9 mV from the resting membrane potential. Note that the spontaneous action potential that occurred following the depolarizing current step had a similar threshold. *B*, the amplitude mode for EPSPs in this cell was 0·5 mV. With an EPSP amplitude mode of 0·5 mV, 18 nearly synchronous EPSPs would be required to activate this basket cell. *B* and *C*, some EPSPs (denoted by asterisks in *C*) in this cell were much larger than 0·5 mV, and the resting membrane potential of the basket cell drifted over about 5 mV. Both of those factors, in addition to the frequent miniature spontaneous EPSPs that basket cells receive, would lower the number of synchronous EPSPs required for action potential generation.

How many inputs must be simultaneously active to fire a basket cell?

Since it appeared that short bursts of action potentials best activated this pathway and since it has been recently reported that principal cells typically make very few contacts onto interneurons (Gulyas *et al.* 1993), we were interested in determining how many simultaneous inputs were necessary to activate a basket cell. Spontaneous EPSPs in basket cells, recorded under current clamp without tetrodotoxin, were frequently encountered and ranged greatly in amplitude (Fig. 13*B* and *C*). Evoked EPSCs from CA3 pyramidal cell inputs and granule cell inputs (Kneisler & Dingledine, 1995) were indistinguishable based on pharmacology, kinetics, or amplitude, but perforant path-evoked EPSCs in basket cells were much slower rising and decaying than those from CA3 pyramidal cell or granule cell stimulation (Kneisler & Dingledine, 1995). Spontaneous EPSPs detected with a somatic recording, therefore, probably arose from inputs from CA3 pyramidal cells and dentate granule cells but not from the perforant path. The amplitude mode of the spontaneous EPSPs in the cell shown in Fig. 13 was 0·5 mV. The threshold for action potential generation was 9 mV more depolarized than the resting membrane potential (Fig. 13*A*). Based on these numbers, up to eighteen synchronous inputs would be necessary to activate this basket cell.

The resting membrane potential of the twelve basket cells examined with potassium-containing electrodes was $-56 \pm 1{\cdot}2$ mV, and their threshold for action potential generation was $-46 \pm 1{\cdot}6$ mV. With an average EPSP amplitude mode of $0{\cdot}4 \pm 0{\cdot}1$ mV ($n = 5$ neurons), basket cells would need to receive, at most, about twenty-five nearly simultaneous unitary EPSPs to fire an action potential. It is important to note that basket cells voltage clamped to −70 mV in tetrodotoxin normally received a high frequency of miniature EPSCs ($3{\cdot}2 \pm 0{\cdot}6$ Hz, $n = 4$ cells) with variable amplitudes ($-7{\cdot}9 \pm 0{\cdot}7$ pA, $n = 4$ cells) and that frequent spontaneous EPSPs contributed to a fluctuation of the 'resting' membrane potential of about 5 mV (see Fig. 13*C*). In addition, some spontaneous EPSPs had amplitudes much larger than 0·4 mV (see Fig. 13*B*). Large amplitude spontaneous input and frequent miniature events could lower the number of synaptic events required to reach firing threshold. The threshold for activation of these basket cells may be overestimated if the dendritic spike threshold was lower than the somatic spike threshold. The appearance of spontaneous action potentials directly from the resting potential (Fig. 13*C*) indicates that action potentials in the cell can be triggered without a 10 mV somatic depolarization. Nevertheless, it appears that the activation of more than a single input to basket cells is required to evoke an action potential. The necessity of several simultaneous EPSPs for basket cell activation is consistent with the observation that basket cells are better activated by pyramidal cell bursts than by individual action potentials.

DISCUSSION

In this study we identified and characterized an excitatory pathway from CA3 pyramidal cells to dentate basket cells. Four main conclusions can be drawn that are important for the network behaviour of the hippocampus. First, visually identifiable basket cells in the dentate gyrus are excited both monosynaptically and polysynaptically by CA3 pyramidal cells. The identification of these new prominent glutamatergic pathways contributes to the growing body of evidence that antiquates the concept of unidirectional flow of information through the hippocampus (Lacaille & Schwartzkroin, 1988; Ishizuka *et al.* 1990; Muller & Misgeld, 1991; Li *et al.* 1994; Scharfman, 1994*a*,*b*; Sik *et al.* 1994).

Second, the net result in the dentate gyrus of activation of CA3 pyramidal cells is increased inhibition of the granule cells, which indicates that CA3 can control one of its major inputs, the mossy fibres, by limiting granule cell excitability. EPSCs in granule cells were not evoked by electrical stimulation of CA3 pyramidal cells or raised extracellular potassium. Indeed, CA3 pyramidal layer stimulation evoked polysynaptic IPSCs in granule cells. Our results, therefore, do not support the assertion based on anatomical evidence (Li *et al.* 1994) that CA3 pyramidal cell axons form excitatory synapses with granule cells or physiological evidence (Scharfman, 1994*a*) that CA3 pyramidal cell firing induces granule cell EPSPs, probably through a polysynaptic pathway involving hilar mossy cells. Scharfman (1994*a*), however, used different, much stronger stimulation conditions; fimbria stimulation induced epileptiform activity in CA3 pyramidal cells bathed in 5 mM potassium and 25 μM bicuculline. In eight experiments we were unable to detect granule cell EPSCs even under those conditions. Both the anatomical and physiological studies, however, were done using adult rats, whereas our studies were performed in neonatal rats. We suggest that in our neonatal preparation the CA3 pyramidal cell axons coursing through the dentate gyrus molecular layer and hilus have dentate basket cell dendrites as one of their targets, since basket cell processes are common in those regions (Fig. 1), and that the net effect of activation of basket cells is granule cell inhibition.

Third, the CA3 pyramidal cell–basket cell pathway is strongly regulated by GABAergic inhibition. A single stimulus given in the CA3 pyramidal cell layer normally evoked either no response or a single short latency EPSC in basket cells. When bicuculline was added to the bath to reduce $GABA_A$-mediated inhibition in the slice, a single stimulus in the CA3 pyramidal layer evoked in basket cells a short latency EPSC followed by numerous other longer latency, polysynaptic EPSCs. These data imply that the polysynaptic projection is normally under strong inhibitory control. The other cells involved in the polysynaptic pathway were not identified but, as discussed above, granule cells were found not to participate. Other cells possibly involved in the polysynaptic circuit include

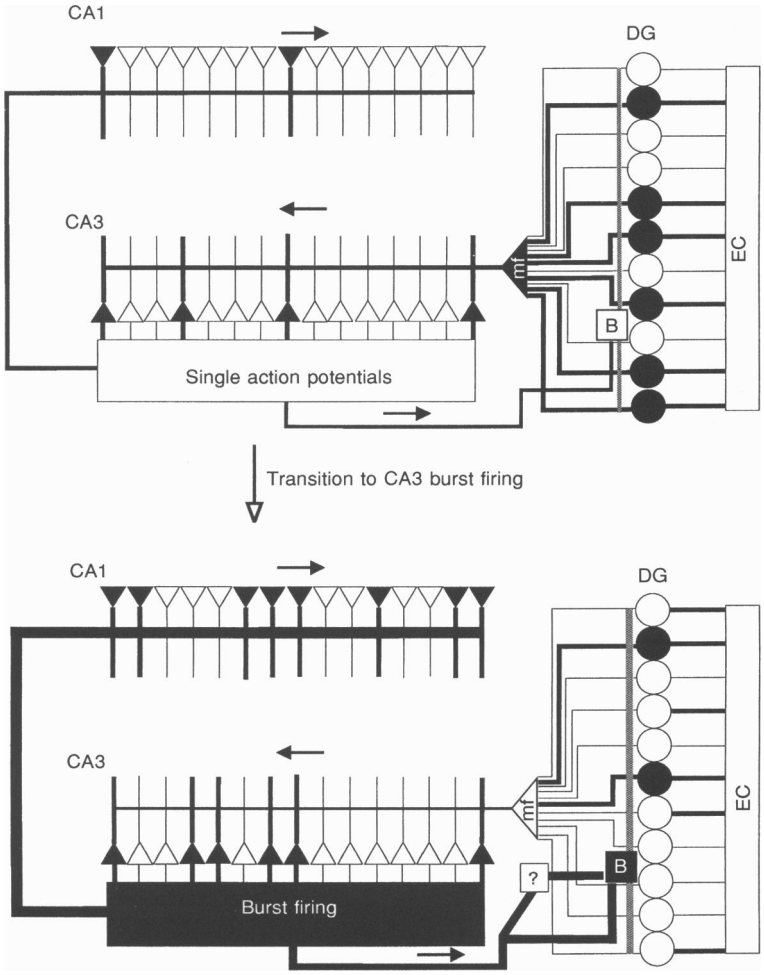

Figure 14. Schematic diagram of basket cell involvement in the regulation of granule cell inhibition by CA3 pyramidal cells

Activated cells are displayed in black, whereas quiet cells are displayed in white. Granule cells, pyramidal cells and basket cells are illustrated as circles, triangles and squares, respectively. Line thickness is in proportion to the amount of synaptic drive propagating from one area to the other. Black lines represent excitatory connections and grey lines represent inhibitory connections. Information flows into the dentate gyrus (DG) via the entorhinal cortex (EC) and continues via the mossy fibres (mf) and Schaffer collaterals to CA3 and CA1, respectively. Information direction is represented by arrows. Information flow from CA3 to the dentate gyrus via the basket cells appears to be best activated by trains of action potentials in CA3 pyramidal cells. CA3 pyramidal cells normally fire single action potentials in response to granule cell input (upper diagram). CA3 output to basket cells would be sparse and weak, thus having little inhibitory effect on granule cells which would not affect flow of information arriving at the dentate gyrus being passed to CA3. However, when CA3 pyramidal cells fire action potentials in bursts (lower diagram), due either to unusual excitatory drive or normal hippocampal processes such as sharp wave generation, basket cells would be more strongly engaged. Excitation of basket cells could then inhibit granule cells, thus raising the threshold for subsequent information transfer from the dentate gyrus. An equivalent input to granule cells during CA3 pyramidal cell burst firing, therefore, would have less impact than one during single action potential firing in CA3 pyramidal cells (compare granule cell output from an identical EC input in the upper and lower diagrams). This alteration of the signal-to-noise ratio of information into the hippocampus may be an essential part of the circuitry necessary to prevent hippocampal seizures and/or aid in new memory formation.

excitatory hilar mossy cells (Scharfman, 1994*a*,*b*) and CA3 pyramidal cells through recurrent excitatory collaterals.

Fourth, the pyramidal cell–basket cell polysynaptic pathway is more strongly activated by a short train of action potentials in CA3 pyramids than by single action potentials. This conclusion is supported by paired recordings between CA3 pyramids and dentate basket cells, by recordings in elevated potassium, by paired-pulse facilitation of the pathway, and by the finding that several excitatory inputs are necessary to provoke basket cell action potentials. These data together support the conclusion that basket cells are better activated by a short train of CA3 pyramidal cell action potentials than by single CA3 pyramidal cell action potentials, presumably as a result of facilitation of the synapse by recent activity.

It is important to consider whether the input to basket cells studied here was solely the result of CA3 pyramidal cell activation. In all experiments using electrical stimulation, the stimulation of the CA3 pyramidal layer was slowly increased to the minimum necessary to evoke an EPSC in a basket cell to reduce the likelihood of stimulus spread to other types of cells. Any stimulus spread from the stimulation site to other neurons, such as hilar mossy cells or granule cells, was inconsequential since in slices in which the CA3 pyramidal layer was physically separated from the dentate gyrus by a knife cut, CA3 pyramidal layer stimulation was incapable of evoking basket cell EPSCs, even at stimulus intensities much greater than those normally used. In addition, recordings from granule cells confirmed that they neither received excitatory synaptic input nor were antidromically activated by CA3 pyramidal layer stimulation. Although we are unable to eliminate completely the possibility that other fibres coursing through the pyramidal cell layer were activated by electrical stimulation of the CA3 pyramidal layer, the pyramids themselves are the most likely source of the input. Indeed, it is clear from paired recordings between basket cells and CA3 pyramidal cells that CA3 pyramidal cell action potentials can excite basket cells.

The implications of this pathway in normal and abnormal hippocampal function are likely to be significant. The CA3 pyramidal cell to basket cell pathway, as mentioned earlier, is most strongly activated by CA3 pyramidal cells firing action potentials in bursts, and the effect of activation of the pathway is increased inhibition of granule cells. Burst firing of CA3 pyramidal cells has been implicated in several hippocampal events including new memory formation (Buzsaki, 1989) and generation and propagation of epileptic seizures (e.g. Traub and Miles, 1991). Each of these issues is discussed further.

Role of the CA3 pyramidal cell to basket cell pathway during hyperexcitability

Synchronous burst firing of large populations of CA3 pyramidal cells can lead to hippocampal seizures. Several investigators have proposed that the dentate gyrus acts as a filter to limit information flowing from the entorhinal cortex into the hippocampus (Walther, Lambert, Jones, Heinemann & Hamon, 1986; Dreier & Heinemann, 1991; Stringer & Lothman, 1992). One role for the so-called 'dentate gate' may be to prevent seizure activity in the more susceptible CA3 and CA1 regions. Although not fully understood, the dentate gate under normal circumstances is thought to be regulated by the excitability of the granule cells, which in turn is controlled by several factors including a high granule cell threshold (about 20 mV from resting potential), strong granule cell spike frequency adaptation, and inhibition of granule cells by local circuit neurons. Input resulting in single action potential firing among CA3 pyramidal cells would weakly excite basket cells, which would contribute weakly to granule cell inhibition (Fig. 14, upper panel). However, strong afferent input that results in CA3 pyramidal cells synchronously firing bursts of action potentials would more strongly excite basket cells; the resulting inhibition of granule cell would reinforce the gate and limit further excitatory input into CA3 (Fig. 14, bottom panel).

In instances of continued extreme excitatory input into the dentate gyrus, the dentate gate is eventually eliminated, resulting in maximal dentate activation (MDA). Once the dentate gate has been opened, arriving excitatory activity is amplified in the dentate gyrus and propagated throughout the hippocampus. Sloviter (1994) has recently proposed that the loss of longitudinally projecting hilar mossy cells following periods of hyperexcitability results in a loss of lateral inhibition to surrounding granule cells by removing excitatory input to basket cells (dormant basket cell hypothesis). This loss of lateral inhibition of granule cells results in the excitation of an abnormally large number of granule cells by a given stimulus, which contributes to further excitability. Since the CA3 pyramidal cell–basket cell pathway may involve mossy cells and/or other CA3 pyramidal cells and since mossy cells and CA3 pyramidal cells have extensive longitudinal projections, the CA3 pyramidal cell to basket cell pathways may also contribute to lateral granule cell inhibition. We propose that the loss of intervening cells in the CA3 pyramidal cell to basket cell pathways contributes to the increased excitability of the hippocampus following periods of hyperexcitability.

Involvement of the CA3 pyramidal cell to basket cell pathway in memory circuits

As described above, CA3 pyramidal cells have the ability to indirectly inhibit granule cells via excitation of basket cells. This ability of CA3 pyramidal cells to control their mossy fibre input may be particularly beneficial during new memory formation. In stage one of the Buzsaki two-stage model of memory (Buzsaki, 1989), excitatory inputs from a subset of granule cells during theta-associated behavioural states converge onto a subset of CA3 pyramidal cells resulting in weak excitation and labile potentiation of

recurrent CA3 pyramidal cell synapses. During stage two, granule cells are silent, but the CA3 pyramidal cells initiate population bursts (sharp waves) which generate long term enhancement of CA3 pyramidal cell recurrent collateral synapses and their target CA1 pyramidal cell synapses. Our results show that a population burst in a subset of CA3 pyramidal cells would excite not only CA1 pyramidal cells but also dentate basket cells. The excitation of basket cells would inhibit granule cells, effectively increasing the signal-to-noise ratio of further input into the hippocampus via the dentate gyrus (Fig. 14). This process may prevent the disruption of new memory formation during stage 2 by suppressing unwanted 'noisy' granule cell inputs when memory is being consolidated in CA3. Interestingly, granule cell silence during sharp waves (stage 2) may be explained by intense basket cell activation by synchronously firing CA3 pyramids (Fig. 14, bottom panel).

In sum, we have described a long-range feedback pathway from CA3 pyramidal cells to dentate basket cells that may function to limit mossy fibre input to CA3 during periods of hyperexcitability and memory consolidation. It will be interesting to determine if the CA3 pyramidal cell to basket cell pathway, like the Schaffer collateral pathway, experiences long term potentiation. It will also be interesting to investigate whether potentiation of this pathway is necessary for adequate representation of signals flowing into the hippocampus via the dentate gyrus.

ALLEN, C. & STEVENS, C. F. (1994). An evaluation of causes for unreliability of synaptic transmission. *Proceedings of the National Academy of Sciences of the USA* **91**, 10380–10383.

BUHL, E. H., HALASY, K. & SOMOGYI, P. (1994). Diverse sources of hippocampal unitary inhibitory postsynaptic potentials and the number of synaptic release sites. *Nature* **368**, 823–828.

BUZSAKI, G. (1989). Two-stage model of memory trace formation: A role for 'noisy' brain states. *Neuroscience* **31**, 551–570.

DREIER, J. P. & HEINEMANN, U. (1991). Regional and time dependent variations of low Mg^{2+} induced epileptiform activity in rat temporal cortex slices. *Experimental Brain Research* **87**, 581–596.

EDWARDS, F. A., KONNERTH, A., SAKMANN, B. & TAKAHASHI, T. (1989). A thin slice preparation for patch clamp recordings from neurones of the mammalian central nervous system. *Pflügers Archiv* **414**, 600–612.

GULYAS, A. I., MILES, R., SIK, A., TOTH, K., TAMAMAKI, N. & FREUND, T. F. (1993). Hippocampal pyramidal cells excite inhibitory neurons through a single release site. *Nature* **366**, 683–687.

HAN, Z.-S., BUHL, E. H., LORINCZI, Z. & SOMOGYI, P. (1993). A high degree of spatial selectivity in the axonal and dendritic domains of physiologically identified local-circuit neurons in the dentate gyrus of rat hippocampus. *European Journal of Neuroscience* **5**, 395–410.

HOUSER, C. R. & ESCLAPEZ, M. (1994). Localization of mRNAs encoding two forms of glutamic acid decarboxylase in the rat hippocampal formation. *Hippocampus* **4**, 530–545.

ISHIZUKA, N., WEBER, J. & AMARAL, D. G. (1990). Organization of intrahippocampal projections originating from CA3 pyramidal cells in the rat. *Journal of Comparative Neurology* **295**, 580–623.

KNEISLER, T. B. & DINGLEDINE, R. (1993). Spontaneous and evoked EPSCs from basket cells in the dentate gyrus. *Society for Neuroscience Abstracts* **19**, 275.

KNEISLER, T. B. & DINGLEDINE, R. (1994). CA3 pyramidal cell input to basket cells in neonatal rat dentate gyrus. *Society for Neuroscience Abstracts* **20**, 400.

KNEISLER, T. B. & DINGLEDINE, R. (1995). Spontaneous and synaptic input from granule cells and the perforant path to dentate basket cells in rat hippocampus. *Hippocampus* (in the Press).

KORN, S. J., GIACCHINO, J. L., CHAMBERLIN, N. L. & DINGLEDINE, R. (1987). Epileptiform burst activity induced by potassium in the hippocampus and its regulation by GABA-mediated inhibition. *Journal of Neurophysiology* **57**, 325–340.

LACAILLE, J. C. & SCHWARTZKROIN, P. A. (1988). Stratum lacunosum-moleculare interneurons of hippocampal CA1 region. I. Intracellular response characteristics, synaptic responses, and morphology. *Journal of Neuroscience* **8**, 1400–1410.

LI, X.-G., SOMOGYI, P., YLINEN, A. & BUZSAKI, G. (1994). The hippocampal CA3 network: An *in vivo* intracellular labeling study. *Journal of Comparative Neurology* **339**, 181–208.

MCNAUGHTON, B. L., SHEN, J., RAO, G., FOSTER, T. C. & BARNES, C. A. (1994). Persistent increase of hippocampal presynaptic axon excitability after repetitive electrical stimulation: Dependence on *N*-methyl-D-aspartate receptor activity, nitric-oxide synthase, and temperature. *Proceedings of the National Academy of Sciences of the USA* **91**, 4830–4834.

MULLER, W. & MISGELD, U. (1991). Picrotoxin- and 4-aminopyridine-induced activity in hilar neurons in the guinea-pig hippocampal slice. *Journal of Neurophysiology* **65**, 141–147.

PATRYLO, P. R., SCHWEITZER, J. S. & DUDEK, F. E. (1994). Potassium-dependent prolonged field bursts in the dentate gyrus: effects of extracellular calcium and amino acid receptor antagonists. *Neuroscience* **61**, 13–19.

POOLOS, N. P., MAUK, M. D. & KOCSIS, J. D. (1987). Activity-evoked increases in extracellular potassium modulate presynaptic excitability on the CA1 region of the hippocampus. *Journal of Neurophysiology* **58**, 404–416.

RIBAK, C. E. & PETERSON, G. M. (1991). Intragranular mossy fibers in rats and gerbils form synapses with the somata and proximal dendrites of basket cells in the dentate gyrus. *Hippocampus* **1**, 355–364.

RIBAK, C. E., VAUGHN, J. E. & SAITO, K. (1978). Immunocytochemical localization of glutamic acid decarboxylase in neuronal somata following colchicine inhibition of axonal transport. *Brain Research* **140**, 315–332.

RUTECKI, P. A., LEBEDA, F. J. & JOHNSTON, D. (1985). Epileptiform activity induced by changes in extracellular potassium in hippocampus. *Journal of Neurophysiology* **54**, 1363–1374.

SCHARFMAN, H. E. (1994*a*). Synchronization of area CA3 hippocampal pyramidal cells and non-granule cells of the dentate gyrus in bicuculline-treated rat hippocampal slices. *Neuroscience* **59**, 245–257.

SCHARFMAN, H. E. (1994*b*). Evidence from simultaneous intracellular recordings in rat hippocampal slices that area CA3 pyramidal cells innervate dentate mossy cells. *Journal of Neurophysiology* **72**, 2167–2180.

SCHARFMAN, H. E., KUNKEL, D. D. & SCHWARTZKROIN, P. A. (1990). Synaptic connections of dentate granule cells and hilar neurons: results of paired intracellular recordings and intracellular horseradish peroxidase injections. *Neuroscience* **37**, 693–707.

SCHARFMAN, H. E. & SCHWARTZKROIN, P. A. (1990). Responses of cells of the rat fascia dentata to prolonged stimulation of the perforant path: sensitivity of hilar cells and changes in granule cell excitability. *Neuroscience* **35**, 491–504.

SERESS, L. (1978). Pyramid-like basket cells in the granular layer of the dentate gyrus in the rat. *Journal of Anatomy* **127**, 163–168.

SERESS, L. & FROTSCHER, M. (1991). Basket cells in the monkey fascia dentata: a Golgi/electron microscopic study. *Journal of Neurocytology* **20**, 915–928.

SERESS, L. & RIBAK, C. E. (1983). GABAergic cells in the dentate gyrus appear to be local circuit and projection neurons. *Experimental Brain Research* **50**, 173–182.

SERESS, L. & RIBAK, C. E. (1990). Postnatal development of the light and electron microscopic features of basket cells in the hippocampal dentate gyrus of the rat. *Anatomy and Embryology* **181**, 547–565.

SIK, A., YLINEN, A., PENTTONEN, M. & BUZSAKI, G. (1994). Inhibitory CA1–CA3–hilar region feedback in the hippocampus. *Science* **265**, 1722–1724.

SLOVITER, R. S. (1994). The functional organization of the hippocampal dentate gyrus and its relevance to the pathogenesis of temporal lobe epilepsy. *Annals of Neurology* **35**, 640–654.

SLOVITER, R. S. & NILAVER, G. (1987). Immunocytochemical localization of GABA-, cholecystokinin-, vasoactive intestinal polypeptide-, and somatostatin-like immunoreactivity in the area dentata and hippocampus of the rat. *Journal of Comparative Neurology* **256**, 42–60.

STEVENS, C. F. (1994). Cooperativity of unreliable neurons. *Current Biology* **4**, 268–269.

STRINGER, J. L. & LOTHMAN, E. W. (1992). Bilateral maximal dentate activation is critical for the appearance of an afterdischarge in the dentate gyrus. *Neuroscience* **46**, 309–314.

TARENISHI, T. & NEGISHI, K. (1994). Double-staining of horizontal and amacrine cells by intracellular injection with lucifer yellow and biocytin in carp retina. *Neuroscience* **59**, 217–226.

TRAUB, R. D. & MILES, R. (1991). *Neuronal Networks of the Hippocampus*. Cambridge University Press, New York.

WALTHER, H., LAMBERT, J. D. C., JONES, R. S. G., HEINEMANN, U. & HAMON, B. (1986). Epileptiform activity in combined slices of the hippocampus, subiculum, and entorhinal cortex during perfusion with low magnesium medium. *Neuroscience Letters* **69**, 156–161.

YAARI, Y., KONNERTH, A. & HEINEMANN, U. (1986). Nonsynaptic epileptogenesis in the mammalian hippocampus *in vitro*. II. Role of extracellular potassium. *Journal of Neurophysiology* **56**, 424–458.

ZUCKER, R. S. (1989). Short-term plasticity. *Annual Review of Neuroscience* **12**, 13–31.

Acknowledgements

This work was supported by research grants from the National Institutes of Health.

Received 12 September 1994; accepted 23 February 1995.